

DESIGN OF AN EFFICIENT ENERGY HARVESTER FROM AMBIENT VIBRATION

A report submitted to Department of
Electrical & Electronic Engineering, (EEE)
BRAC University in fulfillment of the requirements
for thesis work.

Tasfia Rahman → 09 221 117

Syedur Rahman Sakir → 09 221 119

Shawzia Dewan Onna → 09 221 055

(April 2012)

Declaration

We do hereby declare that the thesis titled “DESIGN OF AN EFFICIENT ENERGY HARVESTER FROM AMBIENT VIBRATION” is submitted to the Department of Electrical and Electronics Engineering of BRAC University in partial fulfillment of the Bachelor of Science in Electrical and Electronics Engineering. This is our original work and was not submitted elsewhere for the award of any other degree or any other publication.

Date: 12th April, 2012

Supervisor: DR. MOSADDEQR RAHMAN

Tasfia Rahman
ID: (09 221 117)

Syedur Rahman Sakir
ID: (09 221 119)

Shawzia Dewan Onna
ID: (09 221 055)

Abstract

The aim of this thesis was to design and an efficient energy harvester from ambient vibrations. An energy harvester is merely a device that will convert ambient energy into some usable electrical energy. In this work we designed a vibration energy harvester using electromagnetic transduction mechanism.

The system consists of a fixed (movable) magnet and a movable (fixed) coil attached to a spring. When under vibration, relative motion between the fixed magnet and a moving coil or between the moving magnet and a fixed coil created a time varying flux linkage to the coil, thus inducing an electro-magnetic force. The electrical energy thus extracted from these vibrations need to be stored, using a battery charger circuit, and later on this may be used to drive electronic gadgets, self-powered micro-systems and wireless sensor network.

In this work we designed the electro-mechanical energy harvesting system for optimum performance for a range of vibration energy and frequency, starting from 300-350Hz and studied the impact of difference device parameters, such as, size of the mass (510mg), stiffness of the spring, number of turns and dia of the coil. A charge controller circuit to store the generated electrical energy can be designed for implementation.

INDEX

1. Introduction	9
1.1 – Motivation	
1.2 – Vibration Energy Harvester	
2. Common Vibration Energy Harvesting Techniques:	16
2.1– Electromagnetic Harvester	
2.2- Piezoelectric Energy Harvester	
2.3- Electrostatic Energy Harvesting	
3. Electromagnetic energy harvester	22
3.1-Model 1: Beam Magnet Setup	
3.2-Model 2: Electromagnetic fabrication setup	
3.3-Model 3	
4. Electromagnetic Energy Harvester Model to be used	25
4.1-Target Application and Basic Design Criteria	
4.2-Theoretical Analysis, Modeling and Design Issue	
4.3-The Natural Frequency (ω_n) and the Spring Constant (K)	
4.4-The Damping Co-efficient and The Coil Design	
5. Maximum Power Transfer and the Load Resistance	39

6. Generator Designing Criteria	41
6.1- Input Section	
6.2-Conversion Section	
6.3-Output Section	
7. Estimated Design Specification for Optimum Energy Harvesting	59
8. Efficiency	60
9. Conclusion	61
10. Further Work(Future Plan)	62
11. References	63
12. Appendix	66

Table List

Tables	Page
1. Table I: Sources of energy available in the surrounding which can be trapped for generating electricity.	11
2. Table II: Sources of Micro Energy and their pros and cons	14
3. Table III: The harvested power for each source	15
4. Table IV: Summary of the comparison of various types of energy harvesting mechanisms.	21
5. Table V: This table shows how the length of the beam affects the spring constant and the natural frequency of the beam, and also corresponding changes on maximum stress and deflection	
6. Table VI: Table showing variation of spring constant and natural frequency as mass of the beam changes	50
7. Table VII: The optimized device specifications	59

Figure List

Figure No. and Name	Page
1. Fig 1: Schematic diagram of a piezoelectric energy harvester	19
2. Fig2: Simple diagram of (capacitive) energy harvesting	20
3. Fig3: Beam Magnet Setup	22
4. Fig4: Split and assembled view of the fabricated electromagnetic harvesters	23
5. Fig5: Figure for Model3	24
6. Fig6: Figure for model 4	24
7. Fig7: schematics of the mass spring damper system	25
8. Fig8: A public bus (wheel-side view)	26
9. Fig9: Graphical representation of the variation of a_x , a_y and a_z with types of busses	27
10. Fig10: Mathematical model	29
11. Fig11: electrical equivalent circuit of the lumped element model	30
12. Fig12: Graph showing variation of natural frequency with mass of beam	35
13. Fig13: Graph showing variation of displacement with frequency	36
14. Fig14: Graph showing variation of average power with total damping	37
15. Fig15: Graph showing variation of damping ratio with total damping	38
16. Fig16: complete electrical equivalent circuit for the whole system.	39
17. Fig17: Graph showing the maximum power variation with coil resistance	40
18. Fig18: Graph showing the maximum power variation with damping ratio	41

19. Fig19: Graph showing the variation of Maximum allowable deflection with change in the length of the beam	45
20. Fig20: Graph showing the variation of Natural Frequency with change in the length of the beam	46
21. Fig21: Graph showing the variation of Natural Frequency with change in the mass of the beam	47
22. Fig22: Graphs showing variation of thickness of beam and its effect on max allowable deflection and the natural frequency	48
23. Fig23: Graphs showing variation of width of the beam and its effect on max allowable deflection and the natural frequency	49
24. Fig24: Graph showing variation of output power with varying damping factor	54
25. Fig 25: Variation of output power with change in mass	55
26. Fig26: Variation of electrical damping with (a) Coil Resistance & (b) No. of turns	56
27. Fig27: Variation of electrical damping with (a) Coil Length & (b) Magnetic Flux	57
28. Fig28: Graph showing variation of output power with varying load resistances	58

Acknowledgement

We would like to acknowledge a few people who made this thesis work possible. Firstly we would like to express our deepest gratitude and sincere thanks to Dr. Mosaddequr Rahman, our thesis advisor, without his supervision, strong support and careful criticism we wouldn't have been able to take this thesis so far. He enabled us to develop the core concepts and basics for understanding this topic.

We also express thankfulness to Mr. Supriyo Shafkat Ahmed and Ms. Sanjida Hossain Sabah, who have helped us in the developmental stages of this thesis by sharing valuable expertise and ideas.

We would also like to thank Allah, for helping us in this work, and giving us the ability to do the hard-work and determination that was required for this thesis.

Introduction

1.1 Motivation

Energy harvesting is an active field of research aimed at powering low power wireless systems, self-powered sensors and micro-systems and recharging existing batteries. Renewable energy can be harvested by generating electrical energy from solar, thermal or kinetic energy present within or around the system. Solar cells are excellent energy harvester under direct sunlight, but are limited in application under dim day light condition, in the night and where light has no access, such as in embedded systems. Thermal energy can be converted into electrical energy using seeback effect, but this approach produces energy in the range of a few μW only.

Kinetic energy harvester converts kinetic energy present in the environment into electrical energy. It has already been demonstrated by several groups that the ambient kinetic energy can be easily converted into electrical energy in the μW range. Kinetic energy is typically present in the form of vibration, random displacement of forces and is typically converted into electrical energy using electromagnetic, electrostatic and piezoelectric energy transduction method.

There has been a significant increase in research on energy harvesting techniques. It is the process whereby ambient energy is captured and converted to usable electrical energy and then stored for later use. Ambient energy is natural, non-electrical in nature, and is self-regenerating or renewable.

Most of this research has been focused on technology specific solution. The sources of ambient energy, depends on the applications. The most familiar ambient energy source is solar power. Thermal energy is another ambient energy source [1]. Flow of liquids or gases, energy produced by the human body [2], the action of gravitational fields [3] and tides are other ambient energy source possibilities. By energy harvesting Module this

energy can perform to power a variety of sensor and control circuitry for alternating duty applications.

Necessity of energy harvesting

Among many other advantages the primary reasons for the use of energy harvesting are:

- **Convenience:** Nowadays energy harvesting is essential because of the future scarcity of the natural mineral resources. Energy harvesting is done from those natural resources which are inexhaustible. So that it is more convenient than wall plugs and batteries which are costly and need replacements.
- **Back up energy source:** It can also be used as the backup of the primary sources. Therefore, it will increase the system's reliability and prevent power interruption. Moreover, this energy sources are considered as free form of energy in comparison with fossil fuel. If the energy harvester is designed and installed properly then it will be available throughout the lifetime of the application.
- **Mobility:** Advanced low power VLSI design and CMOS fabrication have reduced power requirement for wireless sensor nodes to the point that the self powered noded are feasible. Harvesting energy form ambient vibrations, wind, heat or light could enable smart device to be functional for an indefinite period.
- **Environmentally Friendly:** Energy harvesting aims to eliminate the dependence on batteries which contains heavy metals that are toxic to living organisms. Furthermore, this technology promises to reduce the dependence on non-renewable energy sources.
- **Production cost:** Business costs for consumers would be reduced in terms of the packaging, development, disposal, longevity, and reuse of those products. For instance, in the use of a cell phone, the cost of a chemical battery and charger would be saved by replacing energy harvester device.

1.2 Vibrational Energy Harvester

Vibration energy available in a wide variety of sources can be conveniently used for potential powering of wireless sensors and low power devices. Data acquired from the Annual Energy Harvesting Workshop suggests some of the potential vibration sources for energy harvesting:

- a. Stiff structures which move on their own. For example: escalators, bridges, refrigerators
- b. Elastic structures which show an elastic deformation of their walls. For example: rotor blades, windmill blades, pumps
- c. Soft structures with very low elastic modulus and deformation ratios. For example: textiles, leather, and piping with internal fluid flow.

Table 1: Sources of energy available in the surrounding which can be trapped for generating electricity.

Human body	Vehicles	Structures	Industrial	Environment
Breathing, blood pressure, exhalation, body heat	Aircraft, UAV, helicopter, automobiles, trains	Bridges, roads, tunnels, farm house structures	Motors, compressors, chillers, pumps, fans	Wind
Walking, arm motion, finger motion, jogging, swimming, eating, talking	Tires, tracks, peddles, brakes, shock absorbers, turbines	Control-switch, HVAC systems, ducts, cleaners, etc.	Conveyors, cutting and dicing, vibrating mach.	Ocean currents, acoustic waves,

Sources of energy harvesting can be classified to two types:

1. **Macro energy sources** – The renewable energy sources which are capable of generating a significant amount of electricity (more like kilowatt to Megawatt). Some patterns are discussed below:

a) Solar energy:

Energy captured from sunlight or room light via photo sensors, photo diodes, or solar panels.

Solar panels are consisting of a number of cells containing a photovoltaic material. 100 mm² photovoltaic cell can scavenge approximately 1mW of average power. Typical efficiency is 10 percent and the capacity factor of photovoltaic sources (the ratio of average power produced to power that would be produced if the sun was always shining) is about 15 to 20 percent.

Applications:

- *Sun bricks*: it is a self contained solar powered device which has two LED lights. If placed in sunlight during the day, it can stay lit up to 8hours.



- *Solar powered security camera*: An outdoor camera solely power by sunlight. This device only transmits A/V when movement is sensed, or else it remains in standby mode to conserve energy.
- *Sol8*: it is a 9.5pound briefcase with two solar panels that generates 13W. This devices can easily run laptops, small electric hand tools, GPRS systems. [4]



b) Wind energy:

Wind turbines are used to convert mechanical energy from wind energy. Wind turbine takes velocity or kinetic energy out of the wind. This mechanical energy is used to

produce electricity. Wind can blow at different speed, so the efficiency will be on inconsistency level. Wind turbines are generally operated at the lower than its best efficiency. So far the efficiency of the wind turbine is 30-40 percent at its best capacity.

Applications:

- *Wind power water harvester:* This device is capable of harvesting the ultimate water from the air. It consists of a wind turbine that is capable of both running a refrigeration system and condensing moisture from it. A four-meter square device could extract an average 7,500 liters of water a day.
- *HyMini charger:[6]* it is a small device with a turbine. If anyone go for a bike or car-ride can attach this device to the vehicle. Then the wind turbines will trickle charge for storing on this device.



2. Micro energy source

Micro harvesting is the system which can produce electricity in scale of micro or miliwatt. This is intended for ultra-low power solution. Some of the Promising sources are discussed below [5]:

Table II: Sources of Micro Energy and their pros and cons

	Advantages	Disadvantages	Application area
<i>photonic</i>	<p>Cost effective.</p> <p>Size effective.</p> <p>Durable.</p> <p>DC power.</p>	<p>Does not work well indoors.</p> <p>Prone to failure by debris.</p> <p>Requires secondary storage for 24/7 uptime</p>	<p>Agriculture.</p> <p>Shipping yards.</p> <p>Outdoor security.</p> <p>Transportation.</p>
<i>Thermal</i>	<p>Works where batteries cannot.</p> <p>Adaptable.</p> <p>Active whenever the object to be measured is active.</p>	<p>Requires large thermal gradients</p> <p>Requires bulky sinks</p>	<p>Monitoring industrial exhaust.</p> <p>Furnaces.</p> <p>Engine/power train.</p>
<i>Vibrational</i>	<p>Has the potential to work anywhere there is machinery, regardless of temperature or illumination.</p> <p>Frequency can be turned for a specific application.</p>	<p>Highly frequency dependent.</p> <p>Requires excellent mechanical coupling.</p> <p>Requires rectification.</p> <p>Currently expensive.</p>	<p>Machine tool monitoring.</p> <p>Pump monitoring.</p> <p>Engine monitoring.</p>

Other Energy sources:

Chemical secretion and biological matters can be the sources for energy harvesting. Tree metabolic energy harvesting is another latest way of energy harvesting. It is a type of bio-energy harvesting. Energy sources which are the direction for future resources are noise, radiation, electro active matters etc.

The chart below shows the approximate amount of energy per unit available from some micro-harvesting sources: [7]

Table III: The harvested power for each source

Energy Source	Harvested Power
<i>Vibration/motion</i>	
Human	4 μ W/cm ² erature
Industry	100 μ W/cm ²
<i>Temperature difference</i>	
Human	25 μ W/cm ²
Industry	1–10 mW/cm ²
<i>Light</i>	
Indoor	10 μ W/cm ²
Outdoor	10 mW/cm ²

Vibration energy harvester requires a transduction mechanism to generate electrical energy from motion and a mechanical system to couple the vibration energy to the transduction process. The mechanical system usually consists of an internal generator, with a suspended mass attached to an inertial frame. The transduction mechanism generates electricity by exploiting the strain within the mechanical system that uses piezoelectric material, or by inducing flow of charge by varying relative position between two plates (electrostatic effect), or by inducing electro-magnetic force in a coil by varying by flux linkage due to relative velocity between the coil and a magnet. In this report, we will explore the design and construction of an efficient energy harvester exploiting electromagnetic transduction method.

2. Common Vibration Energy Harvesting Techniques:

Vibration energy harvesting has become important as devices like sensors are getting smaller and more efficient, requiring less power and has acquired a requirement to have their own powering device. Additionally some batteries has to be made very small and if an alternative charging device can be made, which will charge the battery constantly, it decreases the trouble of less storage capacity.

However, vibration energy harvesting can be of many types, depending on the availability and environment of the vibrational energy. Some of the types are discussed below:

Vibration energy harvesting devices can be either electromechanical or piezoelectric. Due to the lack of availability of piezoelectric material, mostly electromagnetic harvester is used.

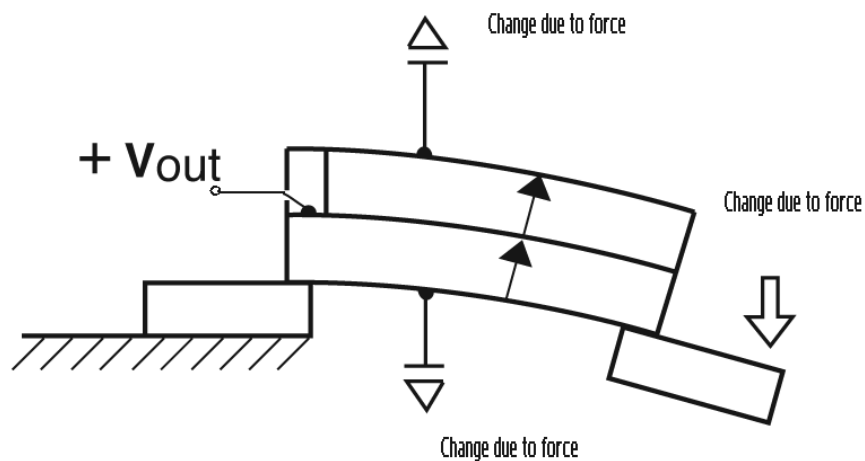
2.1 Electromagnetic Harvester:

In this process, magnetic field is used to produce electric energy. A mass wrapped within a coil can be allowed to oscillate in a magnetic field or a magnet can be used to oscillate inside a coil. In general the coil travels through a varying amount of magnetic flux so it inducing voltage according to Faraday's law. This produces a voltage which is very small (~0.1V) and varying, thus an amplifier circuit has to be used. To do this, many factors can be changed, the magnet strength, number of turns in the coil (more turns means it will cut with the magnetic field lines more), changing the mass or even changing the diameter of the wire which makes the coil. However, each of these parameters is limited by the size. Another important factor is that, it needs no external voltage source to start generating. Typical sources are wind vibration and mechanical vibration (using a cantilever).

2.2 Piezoelectric Energy Harvester:

This method alters mechanical energy into electrical energy by straining or deformation of a piezoelectric material. Deformation of a piezoelectric material causes charge separation across the material, producing an electric field and consequently a voltage drop across it. This voltage drop is almost proportional to the stress applied. The oscillating system is typically a cantilever beam structure with a mass (piezoelectric) at one end of the lever. The voltage produced varies with time and strain, producing an irregular current. Piezoelectric materials can also be used in systems where it is subjected to stress or compression, producing a voltage of around 2~10V.

Piezoelectric energy conversion produces relatively higher voltage and power compared to the electromagnetic system. Piezoelectric materials can separate the electric charges from the crystal lattice which flows through the system. If the piezoelectric material is not short circuited, the applied vibration induces a voltage across the material. This induced voltage is relatively high and the system requires no external voltage source for excitation. It is easy to maintain. However, the material itself is not so very available yet and it depolarizes easily causing less production of voltage at times, leakage voltage is high and it has high output impedance. It is used for harvesting vibration energy where stress or compression is available, for example human body movement, it can be easily placed inside a shoe which will provide enough deformation of the material to produce voltage, as a person walks.



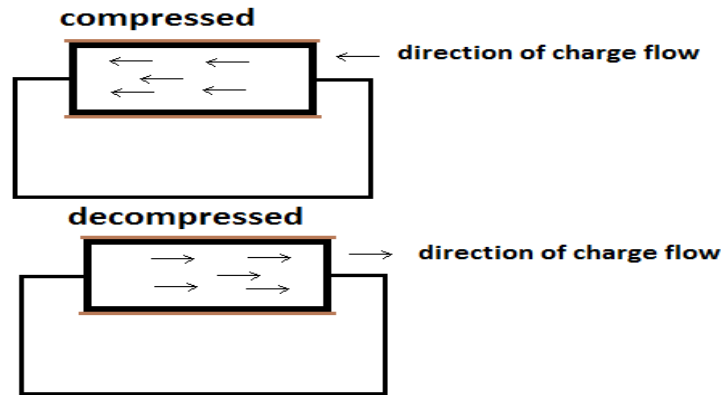


Fig 1: Schematic diagram of a piezoelectric energy harvester

Amongst all piezoelectric materials, PZT is the most efficient, as it is able to convert 80% of the mechanical energy applied to it into electrical energy. PZT is 100 times more efficient than quartz, which is another piezoelectric material.

2.3 Electrostatic (capacitive) energy harvesting:

This type of harvesting is based on the changing capacitance of vibration-dependent variable capacitors. Vibrations separate the plates of an initially charged variable capacitor (varactor), therefore to start generating the system requires an external voltage source, and mechanical energy is converted into electrical energy as both the plates move up and down (mechanical constraints are needed). The produced voltage is relatively high (2-10V). It can be easily worked with MEMS. The system can be placed in a car near to the shock absorber, where the vibration is maximum.

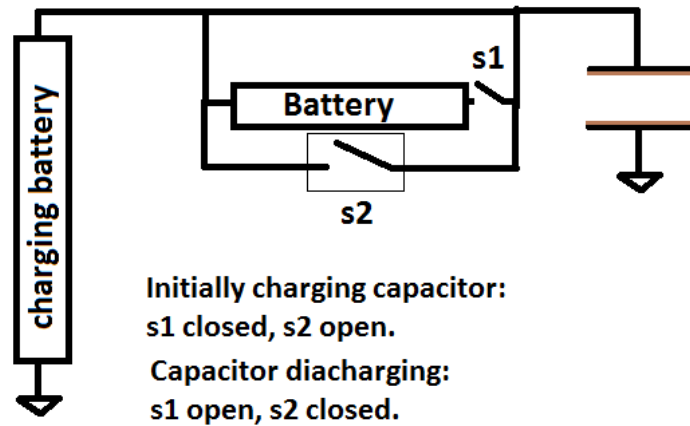


Fig2: Simple diagram of (capacitive) energy harvesting

Table IV: Summary of the comparison of various types of energy harvesting mechanisms.

Type	Advantages	Disadvantages
Electromagnetic	<ul style="list-style-type: none"> • No need of smart material • No external voltage source 	<ul style="list-style-type: none"> • Bulky size • Difficult to integrate with MEMS • Max voltage of 0.1V
Electrostatic	<ul style="list-style-type: none"> • No need of smart material • Compatible with MEMS • Voltage of 2~10V 	<ul style="list-style-type: none"> • External voltage or charge source • Mechanical constraints needed • Capacitive
Piezoelectric	<ul style="list-style-type: none"> • no external voltage source • high voltages of 2~10V • compact configuration • compatible with MEMS • high coupling in single crystal 	<ul style="list-style-type: none"> • depolarization and aging problems • brittleness in PZT • poor coupling in piezo thin film • charge leakage • high output impedance
Magnetostrictive	<ul style="list-style-type: none"> • ultra high coupling coefficient >0.9 • no depolarization problem • high flexibility • suited to high frequency vibration 	<ul style="list-style-type: none"> • non-linear effect • pick-up coil • may need bias magnets • difficult to integrate with MEMS

3. Electromagnetic Energy Harvester:

Structure and operation

There are several models for harvesting vibrational energy using electromagnetic transduction technique. Here examples of models are described below:

3.1 Model 1: Beam Magnet Setup

In this model, a cantilever beam is supported by the housing, and on the beam there are two permanent magnets which act as a mass. There is also a C-shaped core. The arrangement of magnets illustrated is such that the magnetic field distribution in the air gap is uniform.

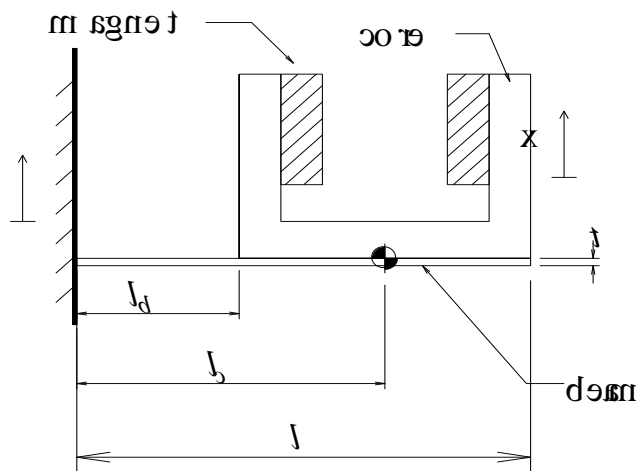


Fig3: Beam Magnet Setup

The C-shaped core serves to provide a path for the magnetic flux causing minimum leakage flux. The coil is made up of copper wires which are enameled. It is placed in the air gap between the magnets, perpendicular to the direction of movement of the mass.

Operating Principle:

As the housing undergoes vibration, a mechanical input force is experienced. Due to this, the mass moves relative to the housing, and energy is stored in the system. The motion is sinusoidal in amplitude and causes a rate of change of flux linkages in the coil. This induces a motional emf on the coil in accordance to Faraday's Law. This has a max useful power output of 0.53mW.

3.2 Model 2: Electromagnetic fabrication setup

This structure is a stacked layer of housing, coil, spacer, and mechanical resonator. Mechanical resonator is 50 μm thick polyimide film; on each side of this film a 35 μm thick layer of copper is electro-deposited.

Two permanent magnets are magnetically attached to both sides of the flexible parts to generate the required magnetic field. The magnets also act as mass. These are 5mm in diameter and 2mm in thickness.

Two copper wire wound coils are used as electrical transducers that will convert the deflection of the resonator into an electrical signal.

Each coil has inductance = 842 μH

And resistance = 10.7 Ω

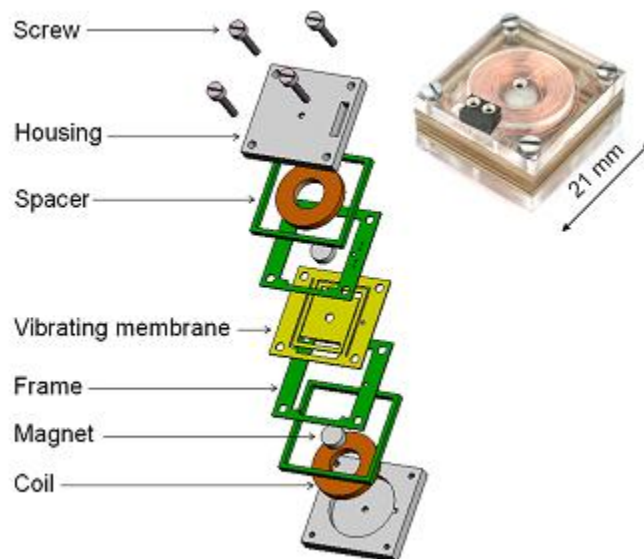
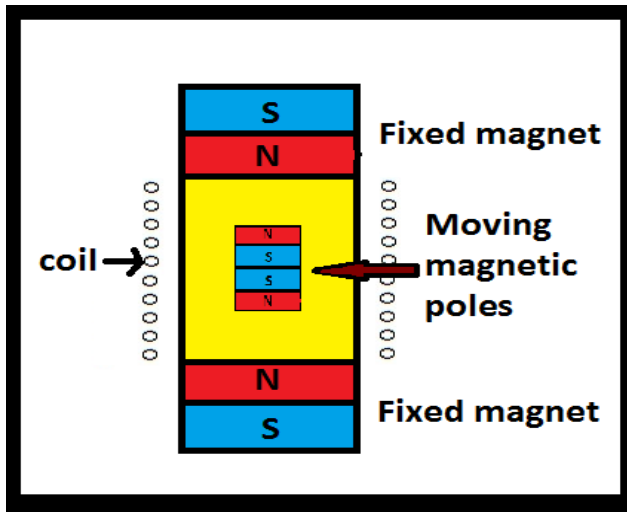


Fig4: Split and assembled view of the fabricated electromagnetic harvesters

This setup from the work of Bouendeu, Greiner, PJ Smith and Korvink has a max power output of 356 μW when connected to a load of 40 Ω , power density of 22 $\mu\text{W/g}$ and weight of 8.12 g

3.3: Model 3:

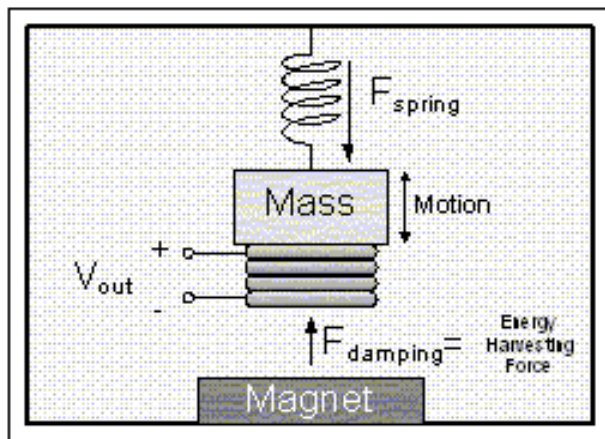


In this model there are two magnets fixed at both ends of the generator tube. A middle magnet is free to move, but it is suspended between both fixed end magnets due to the repulsive force exerted by both fixed end magnets. A coil is wrapped around the outside of the tube, so that when the tube is vibrated, the middle magnet vibrates up and down, and

Fig5: Figure for Model3

then a voltage is induced. For such a system, the generated power varies from 0.3 – 800 μ W. When the tube is vibrated the middle magnet vibrates up and down, and a voltage will be induced in the coil.

3.4: Model 4:



A coil attached to the oscillating mass moves through a magnetic field that is obtained by a stationary magnet. The coil travels through a varying amount of magnetic flux, inducing a voltage according to Faraday's law. The induced voltage is small and must therefore be increased to viably source energy. Methods to increase the

Fig6: Figure for model 4

induced voltage include using a transformer, increasing the number of turns of the coil, and/or increasing the permanent magnetic field. However, each is limited by the size constraints of a microchip.

4. Electromagnetic Energy Harvester Model to be used:

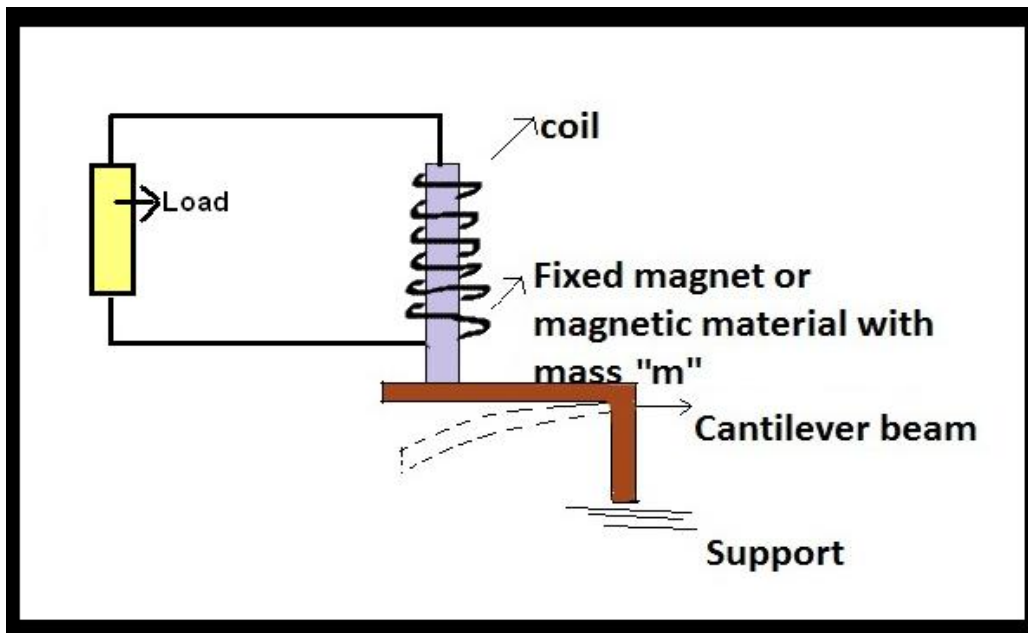


Fig7: schematics of the mass spring damper system

The above system displays a cantilever beam on a fixed support. Mounted on the cantilever beam is a permanent magnet with mass 'm'. Wrapped around the magnet is a coil and with it is an ammeter attached to detect the induced current into the system. As the system experiences any vibration the magnet moves up and down due to the springiness of the cantilever beam. Due to this motion, there is a rate of change of magnetic flux linkages and an induced emf can be found in the system. Our goal is to harvest this energy into power small devices.

Attractive and repulsive forces are used to tune the device to resonance frequencies that are either greater or less than the un-tuned resonance frequency of the device. For the commercial emergence of energy harvesters, they should be working over a wide range of frequencies. For a mass spring damper system, to alter the natural frequency of the harvester we have to change the stiffness or mass associated with it. Stiffness of the device is dependent on the length, width, thickness and elastic modulus of the vibrating beam structure.

4.1: Target Application and Basic Design Criteria:

Mounted on the wheel side of a public bus:

The energy harvester generator can be made compact and mounted on the wheel side of a public bus, attached to a battery charger circuit. This connected with a low power device such as a wireless sensor node, or low power fans or lights, or even charging the other electronics on the bus, can be another target application.

As the vehicle is subjected to bumps on the roads or sudden jerks, etc, there will a vibration energy, and due to passengers being present, there will be somewhat constant vibration force in the vehicle.

This can be used to power the energy harvester designed and can be used to power low power devices.



Fig8: A public bus (wheel-side view)

To calculate the amount of vibration experienced by the bus:

From the work of Ana Picu to determine the ‘Whole Body Vibration Analysis for Bus Drivers’ it is possible to determine the amount of vibration experienced by the generator in the bus.

The whole body vibration can be measured at the driver’s seat on the 3axes x, y and z from the center of the human body. The factor to consider could be the quality of the road the bus is journeying through, for example asphalt, macadam or pavement.

The whole body vibration can be measured using a MAESTRO Virbo-meter produced by a 0.1dB-Metravib and a triaxial accelerometer. The accelerations generated by vibrations can be calculated using the weight factors set by ISO 2631.

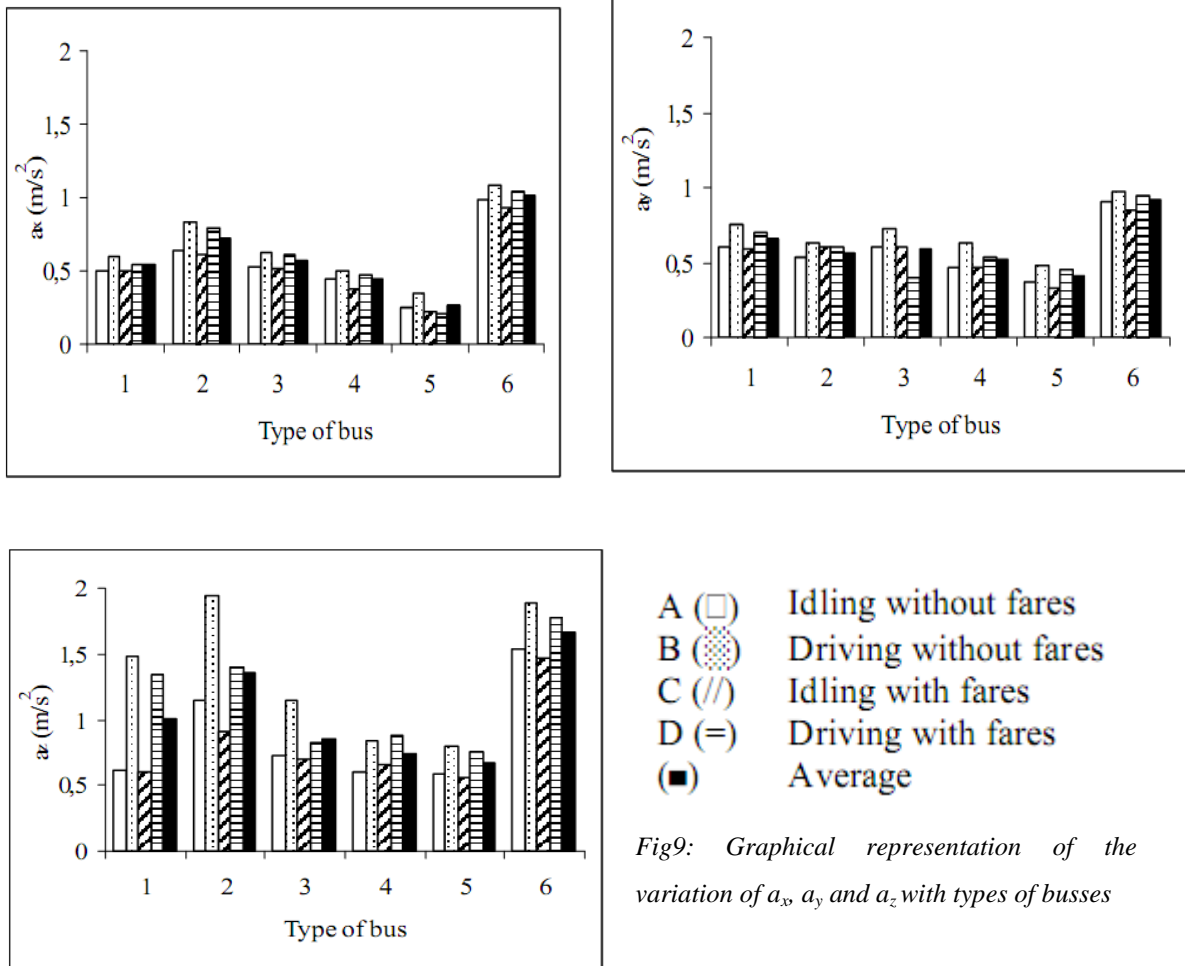


Fig9: Graphical representation of the variation of a_x , a_y and a_z with types of busses

4.2: Theoretical Analysis, Modeling and Design Issue:

The basic vibration energy harvester can be represented by a mass m (usually the magnet) mounted on a spring (usually the cantilever beam), with spring constant k , which vibrates when subjected to an external vibration.

Comparing different approaches to vibration-based generation and for estimation of maximum possible power density that a given vibration source can theoretically apply. The only parameter that distinguishes different technological approaches is the Coupling Coefficient (k).

The theory demonstrates that for any type of generator, the power output depends on:

- the system coupling coefficient
- the quality factor of the device
- the density of the generator defined as the proof mass, divided by the entire generator size
- degree to which the electrical load maximizes power transmission

The power output also is dependent on the magnitude and frequency of the input vibrations.

Estimates of maximum potential power density range from 0.5 to 100mW/cm³ for the range of vibrations ranging from 1 to 10m/s² at frequencies of 50 to 350Hz.

The schematic setup of the model to be used has been illustrated in this report. Following is the mathematical modeling for the set up.

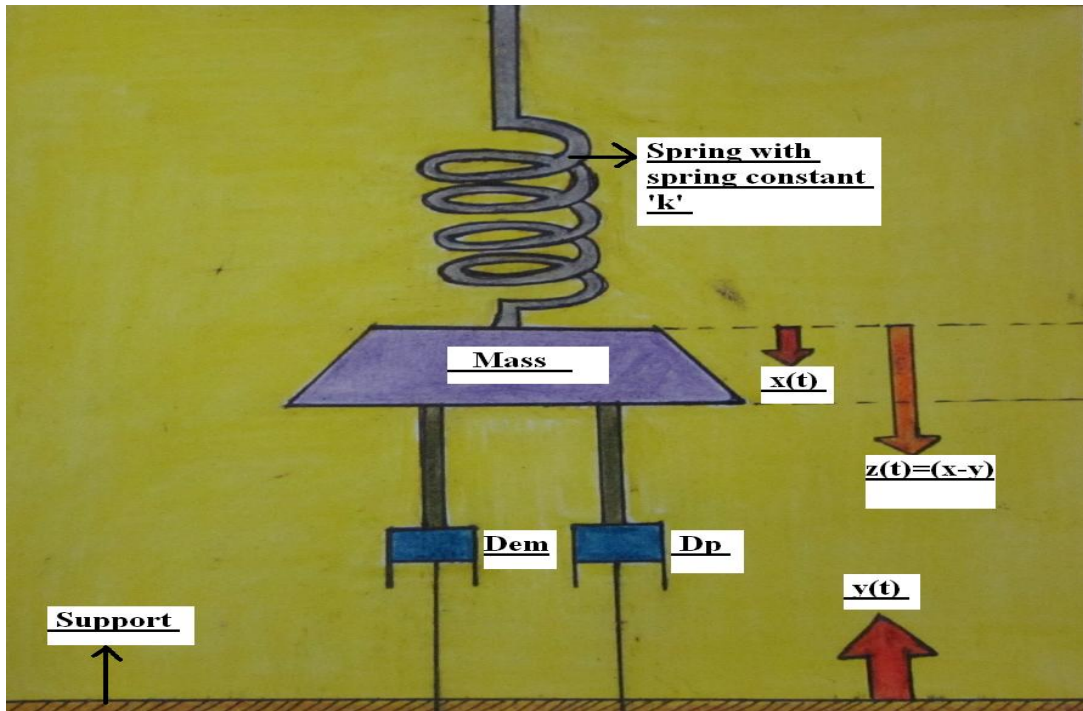
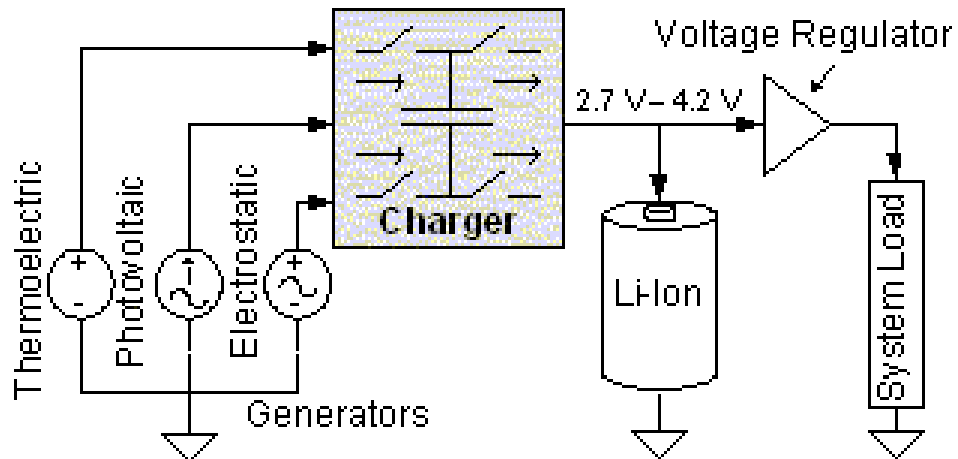


Fig10: Mathematical model

An Electrical Diagram of the Energy Harvester:

[Diagram obtained from google]



Using this mathematical model, the electrical equivalent model can be obtained, shown below. This electrical model consists of a power source, and equivalent electrical components for mass, spring and dashpot represented by inductor, capacitor and resistor respectively. The equivalent electrical model is shown below.

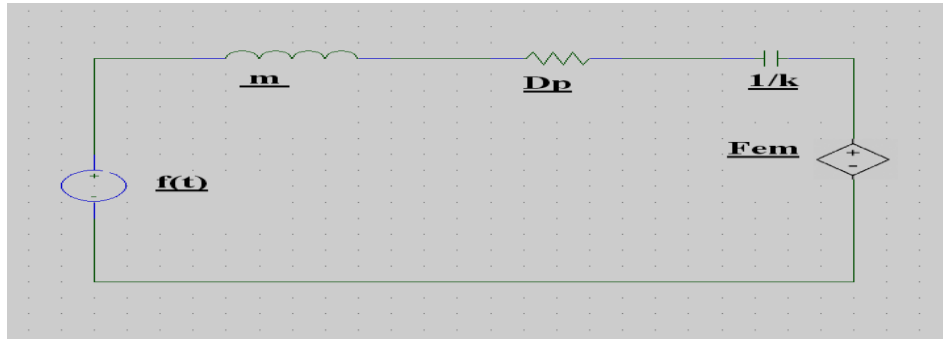


Fig11: electrical equivalent circuit of the lumped element model

Here the basic equation of motion of the mass relative to the housing when driven by a sinusoidal vibration force ($F=ma$) is given by the second order differential equation:

$$m \frac{d^2x}{dt^2} + D_p \frac{dx}{dt} + kx = F_o \sin \omega t - F_{em} \text{-----(1)}$$

And the power source of the electrical equivalent model may be represented as:

$$f(t) = F \sin \omega t \text{-----(2)}$$

The components of equation (1) are as follows:

Here,

$$\bar{x} = \frac{dx}{dt}$$

Where,

x = displacement of the mass

y = displacement of the frame

$(x-y)$ = relative displacement of between the mass and frame

F_{em} = emf due to current in the coil

D_p = Damping due to air resistance

Setting $z = x - y$ in the above equation, we get

$$m \frac{d^2}{dt^2} (z + y) + D_p \frac{dz}{dt} + kz = f(t) - F_{em}$$

$$m \frac{d^2 z}{dt^2} + D_p \frac{dz}{dt} + kz = f(t) - F_{em} - m \frac{d^2 y}{dt^2} \quad (2)$$

Let $y = Y \sin \omega t$,
we get,

$$\frac{d^2 y}{dt^2} = -\omega^2 Y \sin \omega t \quad (3)$$

The retarding emf force F_{em} is given by

$$\begin{aligned} F_{em} &= \left(N \frac{d\phi}{dz} \right)^2 \frac{1}{R_C - R_L - j\omega L_C} \frac{dz}{dt} \\ &= D_{em} \frac{dz}{dt} \end{aligned} \quad (4)$$

Here

$$D_{em} = \left(N \frac{d\phi}{dz} \right)^2 \frac{1}{R_C - R_L - j\omega L_C}, \text{ is the damping due emf force.}$$

In the above equation,

N is the number of turns of the coil,

ϕ is the flux linkage to the coil,

R_C is the coil inductance resistance,

L_C is the coil inductance and

R_L is the load resistance.

Substituting (3),(4) in (2), we get

$$m \frac{d^2 z}{dt^2} + D_p \frac{dz}{dt} + kz = f(t) - D_{em} \frac{dz}{dt} + \omega^2 Y \sin \omega t$$

Rearranging the terms,

$$m \frac{d^2z}{dt^2} + D_T \frac{dz}{dt} + kz = (F + \omega^2 Y) \sin \omega t \quad (5)$$

Here $D_T = D_p + D_{em}$ is total damping of the system.

The steady state solution of the above equation is given by,

$$z = Z \sin(\omega t - \varphi)$$

$$\text{Where, } Z = \frac{F + m\omega^2 Y}{\sqrt{(k - m\omega^2)^2 + D_T^2 \omega^2}} \quad (6)$$

$$\text{and } \varphi = \tan^{-1} \frac{D_T \omega}{k - \omega^2 m} \quad (7)$$

The power delivered can be derived from:

$$P_{av} = \frac{m \xi_T Y^2 \left(\frac{\omega}{\omega_n}\right)^3 \omega^3}{\left[1 - \left(\frac{\omega}{\omega_n}\right)^2\right]^2 + \left[2\xi_T \left(\frac{\omega}{\omega_n}\right)\right]^2}$$

Where:

$$\xi_T = \frac{c_T}{2m\omega_n}$$

$$P_{av} = \frac{mY^2\omega_n^3}{4\xi_T}$$

$$A = \omega^2 Y$$

$$c_T = 2m\omega_n \xi_T$$

$$P_{av} = \frac{(mA)^2}{2c_T}$$

$$Q_T = \frac{\omega_n m}{c_T} = \frac{1}{2\xi_T}$$

Where Q_{OC} is the Q-factor, i.e. $1/2\xi_P$ and Q_E is equal to $1/2\xi_T$

$$\frac{1}{Q_T} = \frac{1}{Q_{OC}} + \frac{1}{Q_E}$$

$$P_{av} = \frac{m\omega_n^3 Y Z_{max}}{2}$$

$$P_{avelec} = \frac{m\xi_E Y^2 \omega_n^3}{4(\xi_P + \xi_E)^2}$$

$$P_{avelec} = \frac{mY^2 \omega_n^3}{16\xi_P}$$

$$P_{L \max} = \frac{mY^2\omega_n^3}{16\xi_P} \left(\frac{R_{load}}{R_{load} + R_{coil}} \right)$$

N is the number of turns in the generator coil

l is the length of the coil

B is the flux density to which it is subjected.

R_L is the load resistance

R_{coil} is the coil resistance

$j\omega L_{coil}$ is the coil inductance.

$$C_E = \frac{(NlB)^2}{R_L + R_{coil} + j\omega L_{coil}}$$

4.3 The Natural Frequency (ω_n) and the Spring Constant (K)

As the energy is extracted from the relative motion between the mass and the coil which is attached to the frame, maximum energy can be extracted when the excitation frequency (ω) matches the natural frequency w_n of the spring-mass system, given by

$$w_n = \sqrt{k/m} \quad (8)$$

Simulating a graph for eqn (8), with the frequency on the y-axis and mass on the x-axis shows the following:

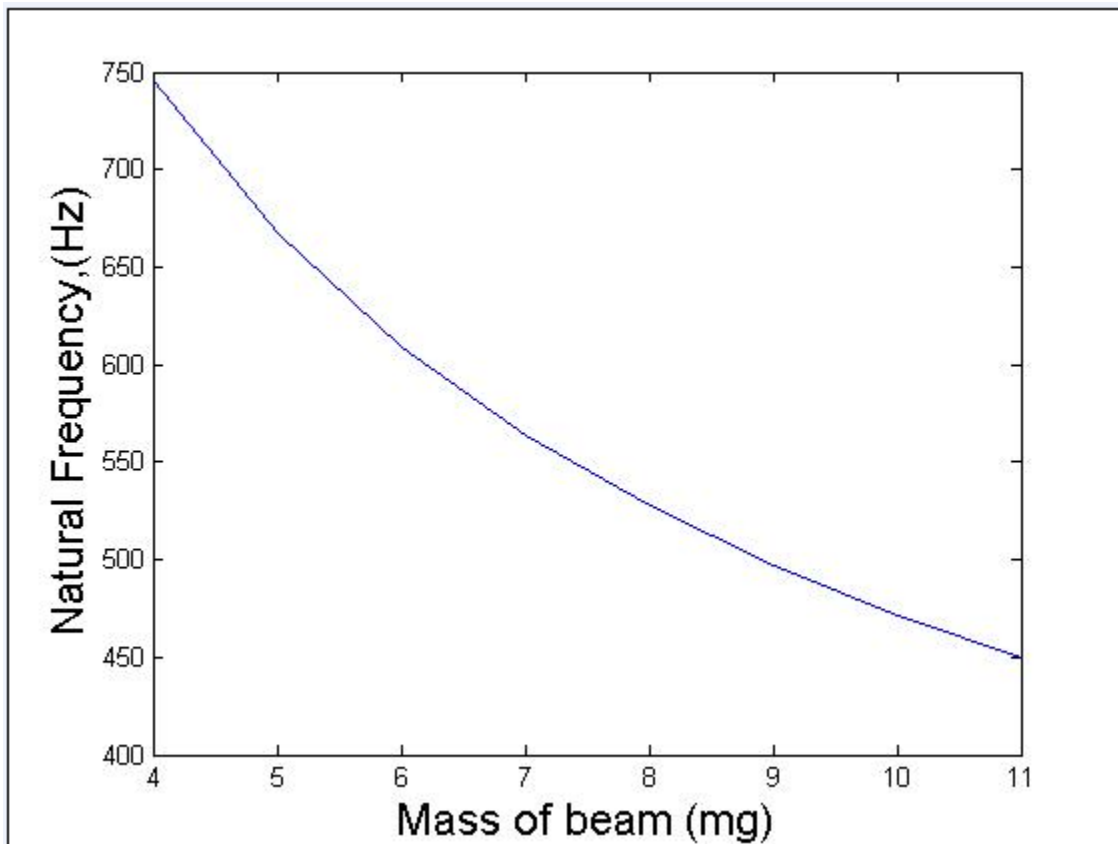


Fig12: Graph showing variation of natural frequency with mass of beam

The trend shows as that the mass of the beam increases, the natural frequency increases.

At this frequency, the relative displacement Z is maximum as can be seen from equation 6

$$Z = \frac{F + m\omega^2 Y}{D_T \omega} \quad (9)$$

It is obvious from the above equation the stiffness of the spring, which in this case is the cantilever beam and the mass of the magnet have to be properly adjusted so as to match the excitation frequency for maximum output. Further, the damping co-efficient also has to be kept to a minimum for maximum z according to equation 9.

Plotting a graph for “ z ”, the displacement of beam on the y-axis with respect to change in frequency in the x-axis gives the following graph:

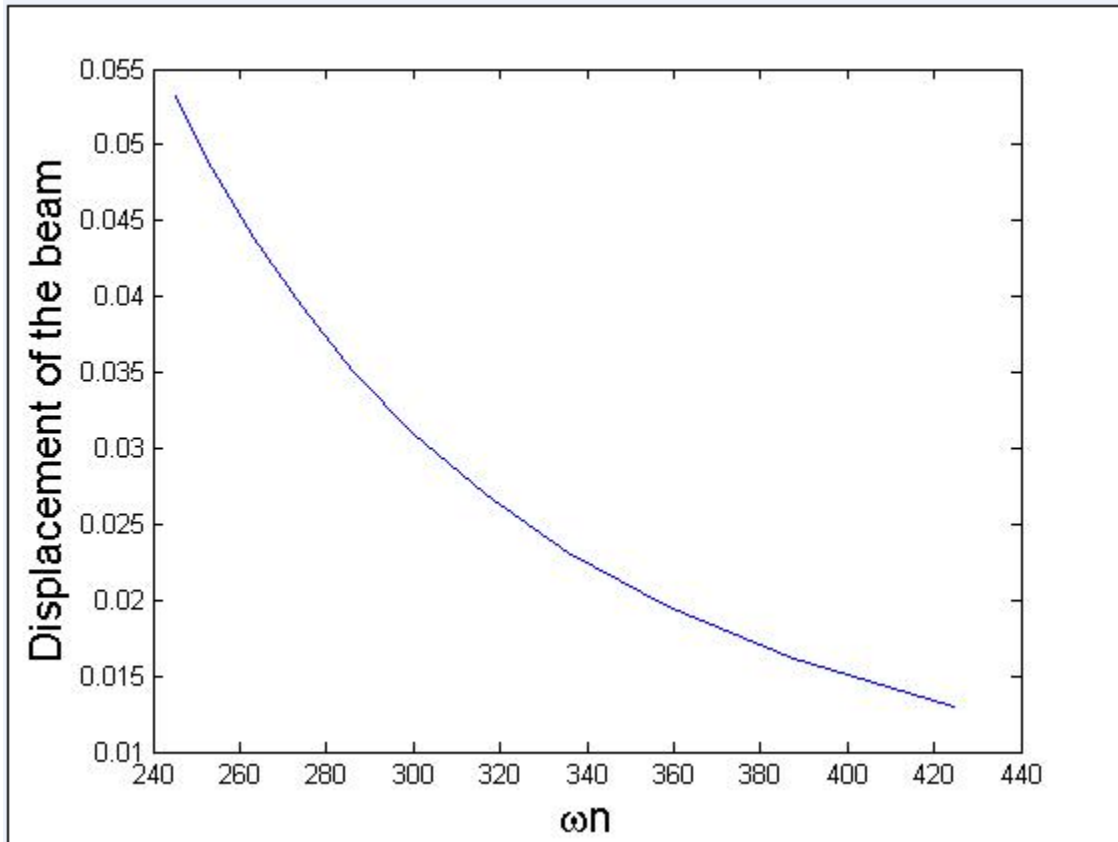


Fig13: Graph showing variation of displacement with frequency

The graph pattern shows that as frequency increases the displacement slowly decreases.

4.4 The Damping Co-efficient and The Coil Design

The average generated power is given by,

$$P_{av} = \frac{1}{T} \int_0^T D_{em} \left(\frac{dz}{dt} \right)^2 dt$$
$$= D_{em} \frac{(F+m\omega^2Y)^2}{2(D_p+D_{em})}$$

From this equation, it can be shown that the maximum average power occurs at,

$$D_{em} = D_p$$

A variation of the total damping with respect to the average power is as shown below:

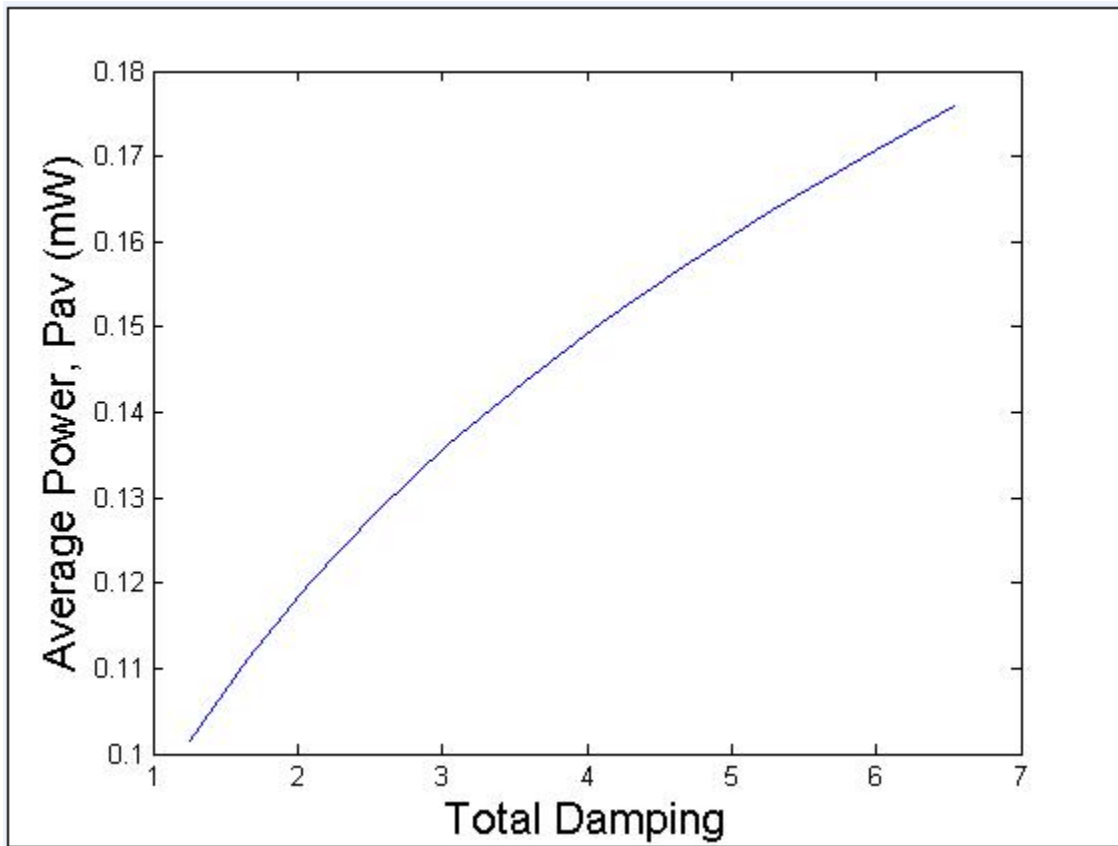


Fig14: Graph showing variation of average power with total damping

The graph shows that as the total damping will decrease the average power obtained will increase.

So, the objective of the generator design should be to make the electromagnetic damping equal to the parasitic damping. This can be achieved by choosing appropriate values of load and coil resistance, number of turns of the coil and the magnetic flux linkage, according to equation 4, Flux linkage to the coil again depends on the number of turns(N) of the coil, length of one turn (l) and the flux density (B).

The graph below shows a variation of the Damping ratio with the total damping, and from simulation it is visible that as the total damping increases the damping ratio also increases almost linearly.

The shape is as follows:

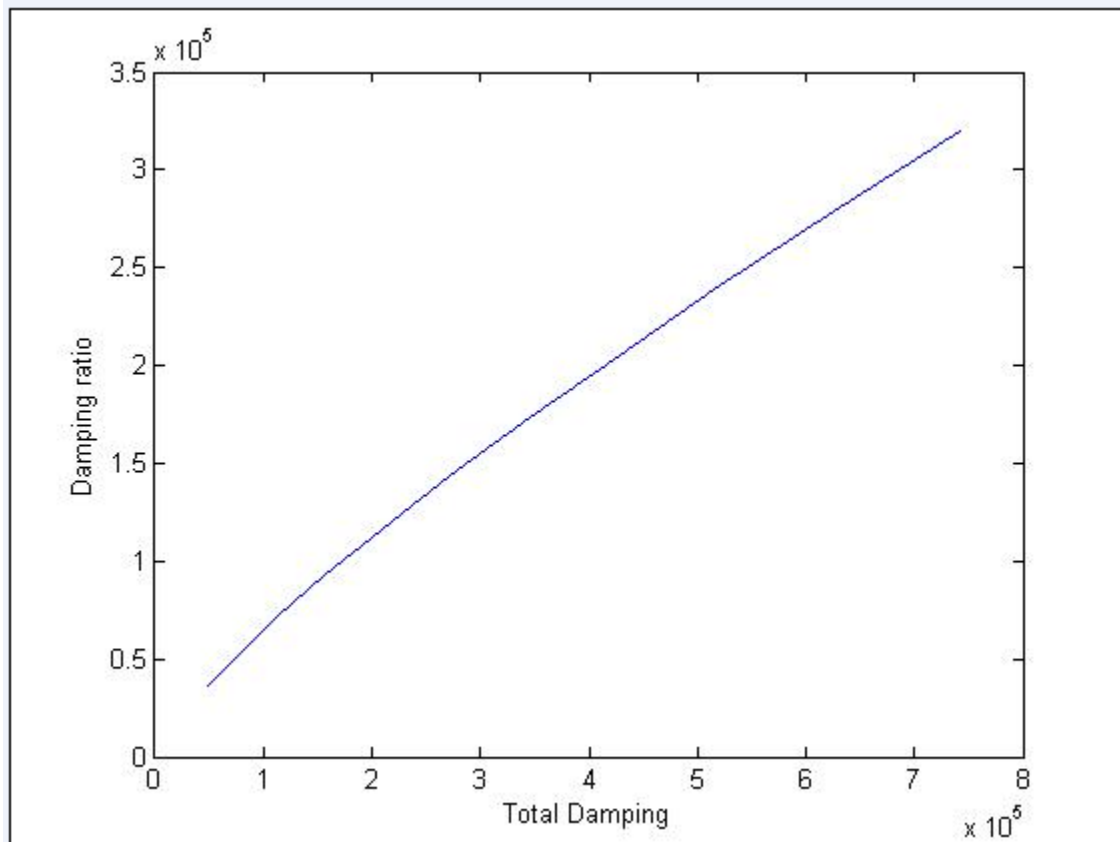


Fig15: Graph showing variation of damping ratio with total damping

5. Maximum Power Transfer and the Load Resistance

Further, to transfer the generated power efficiently to the load, load resistance should match with the output impedance of electrical equivalent circuit of the whole system consisting of the mass-spring-damper, the electromagnetic transduction and the load is shown below:

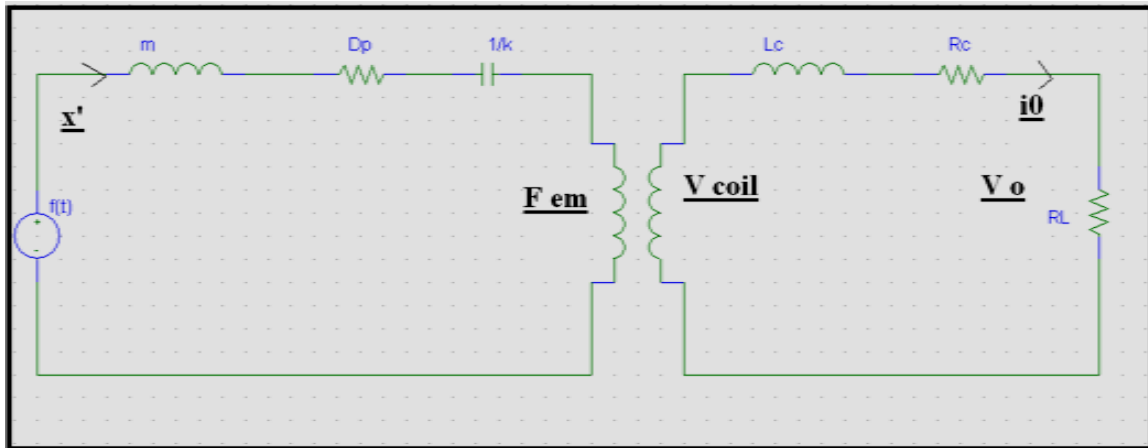


Fig16: complete electrical equivalent circuit for the whole system.

The transformer represents the transduction of energy from magnetic domain to electrical domain. The above circuit can be used to design for maximum power transfer. We plan to do simulation using MATLAB and PSpice to find optimum parameters for this circuit and use it in our target applications.

Simulating the eqn:

$$P_{L\ max} = \frac{mY^2\omega_n^3}{16\xi_P} \left(\frac{R_{load}}{R_{load} + R_{coil}} \right)$$

We obtain a graph of maximum power with variation of coil resistance. As the coil resistance increases the maximum power obtained decreases.

So for designing we will aim for a low coil resistance.

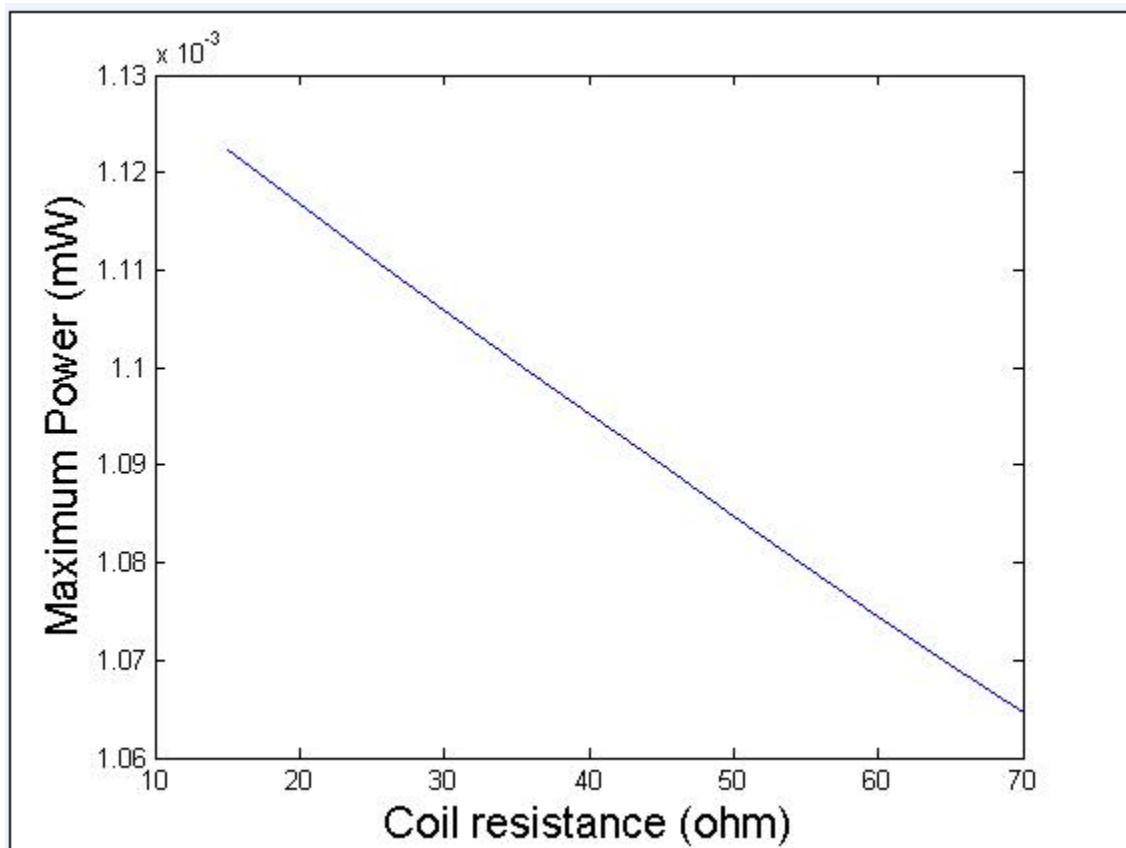


Fig17: Graph showing the maximum power variation with coil resistance

We obtain a graph of maximum power with variation of damping ratio. As the damping ratio increases the maximum power obtained decreases.

So for designing we will aim for a low damping value.

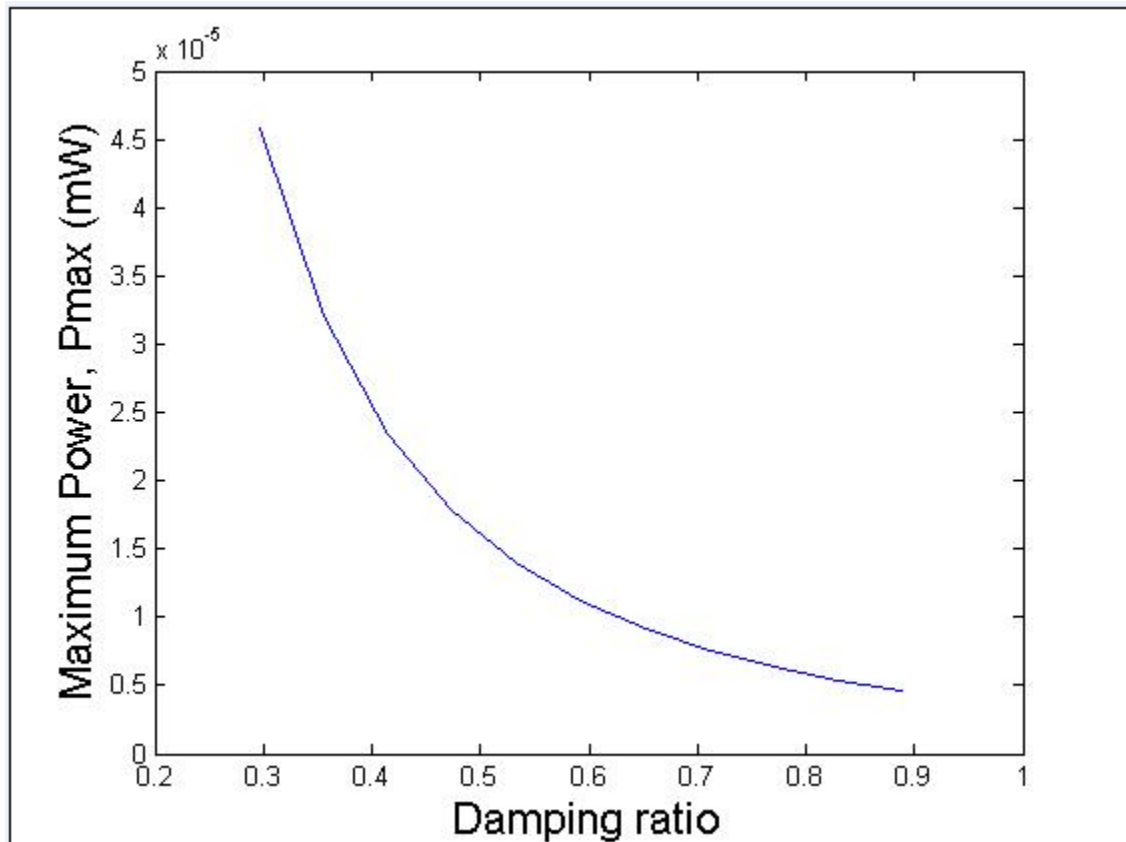


Fig18: Graph showing the maximum power variation with damping ratio

6. Generator Designing Criteria:

Our research continues to search for efficient ways of constructing an energy harvester. We will try to use simulation to design a device that can provide us with the maximum output power. The layout of the work we intend to do is as follows:

- Obtain accurate analytical model that fully describes the system.
- Carry out simulation to optimize different parameters required for efficient energy harvesting.
- Construct the energy harvesting device according to the device parameters obtained from the simulation results.

The work will consist of mainly three segments:

- (i) Input Section: Determining the input parameters of the generator that will be used. This will comprise of the frequency and amplitude of the vibration that the generator will be subjected to.
- (ii) Conversion Section: Here the mechanical displacement will be converted into electrical energy. The mode of conversion used here will be electromagnetic induction. The details and parameters will be discussed in this section.
- (iii) Output Section: This will discuss the load parameters and the power transfer respective to input situations.

6.1: Input Section:

For the input side of our generator we are using a mass spring dashpot system. This mechanical part can be modeled by stainless steel cantilever beam, one end fixed to the housing the other end is free. On the free side a magnet is mounted on top of the cantilever.

To calculate the maximum allowable deflection the following values need to be calculated.

Firstly, we know,

$$y_{\max} = \frac{2L^2}{3Et} \sigma_{\max}$$

Where, y_{\max} is the maximum allowable deflection

E is Young's modulus

t is the thickness, considered as 0.2mm

L is the length of cantilever, considered as 11mm

σ_{\max} is the maximum stress

To calculate maximum stress

$$\sigma_{\max} = \frac{FLt}{2I}$$

Where,

F is the vertical applied force

$$= mg \text{ (m=510mg)}$$

Therefore, $F=5 \times 10^{-2}$ N.

Also we know, I= moment of inertia can be expressed as:

$$I = \frac{Wt^3}{12} \quad (W=3\text{mm and } t=0.2\text{mm})$$

$$= 2 \times 10^{-15}$$

$$\sigma_{\max} = \frac{FLt}{2I}$$

$$= 2.75 \times 10^7$$

The maximum allowable deflection is $y_{\max} = \frac{2L^2}{3Et} \sigma_{\max}$

$$= 5.54 \times 10^{-5} \text{ mm}$$

The spring constant (k) is the ratio between force and the deflection,

$$k = \frac{3EI}{L^3}$$

$$= 901.58$$

The equation of motion for vibration can hence be presented as:

$$m \frac{\partial^2 y}{\partial t^2} + ky = 0$$

Simulating the input section:

The following graphs show the how the parameters can be varied to obtain desired expectations for the generator.

The graph shows how the length of the beam affects the maximum allowable deflection for the stainless steel cantilever beam used in the construction of the energy harvester.

Using the equation,

$$y_{\max} = \frac{2L^2}{3Et} \sigma_{\max}$$

Simulation done illustrates that as the length of beam increases, the maximum allowable deflection tends to increase. Here the graph shows Maximum allowable deflection on the y-axis and length of the beam on the x-axis.

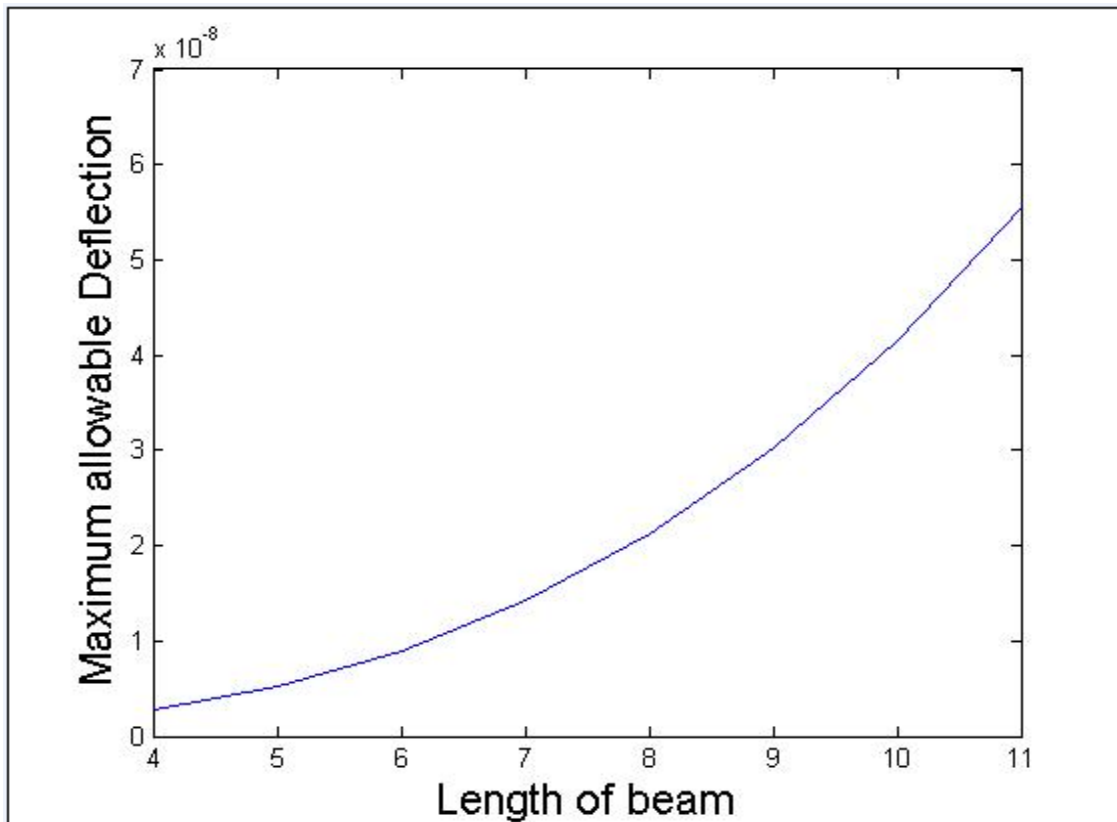


Fig19: Graph showing the variation of Maximum allowable deflection with change in the length of the beam

This second graph shows the variation of natural frequency with the length of the beam, and shows that as the length of the beam increases, the natural frequency tends to decrease.

The y-axis shows the natural frequency whereas the x-axis shows the length of the beam. Depending on the generator size and construction demands, an optimum length needs to be chosen for the cantilever beam construction.

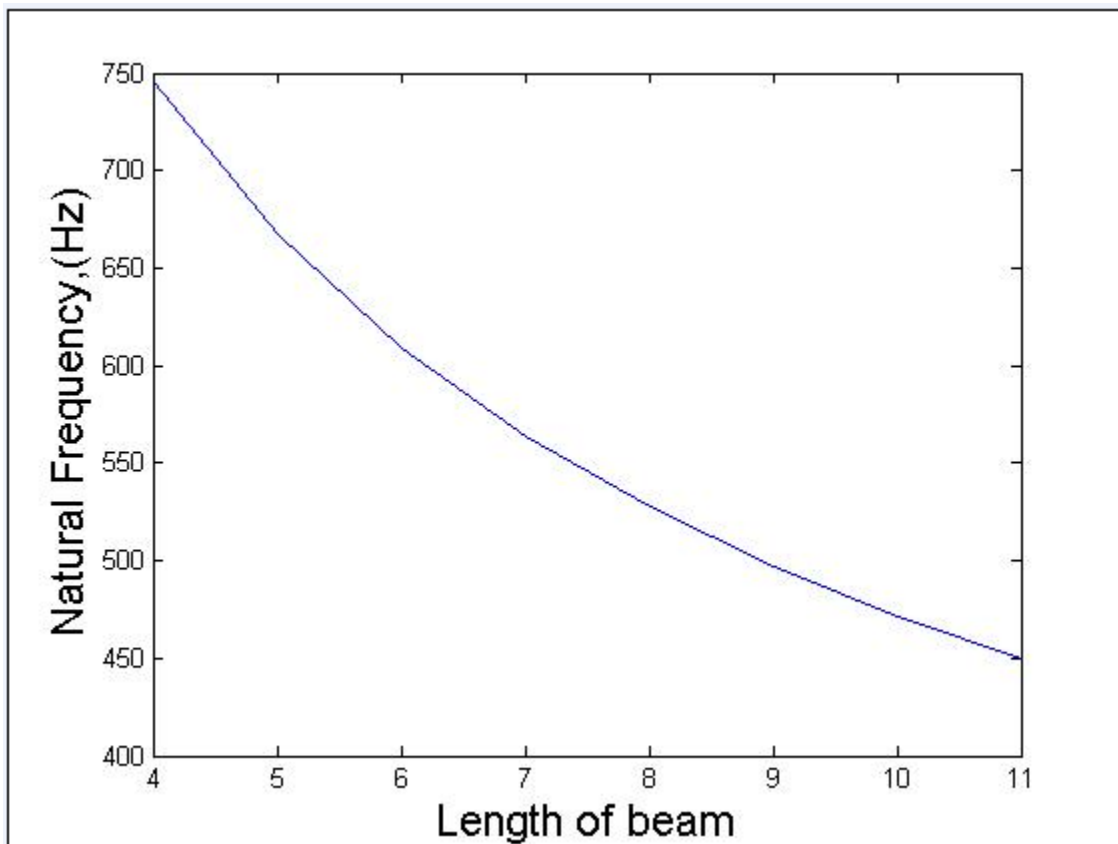


Fig20: Graph showing the variation of Natural Frequency with change in the length of the beam

This third graph shows the variation of natural frequency with the mass of the beam, and shows that as the mass of the beam increases, the natural frequency tends to decrease.

The y-axis shows the natural frequency whereas the x-axis shows the mass of the beam. Depending on the generator size and construction demands, an optimum mass needs to be chosen for the cantilever beam construction.

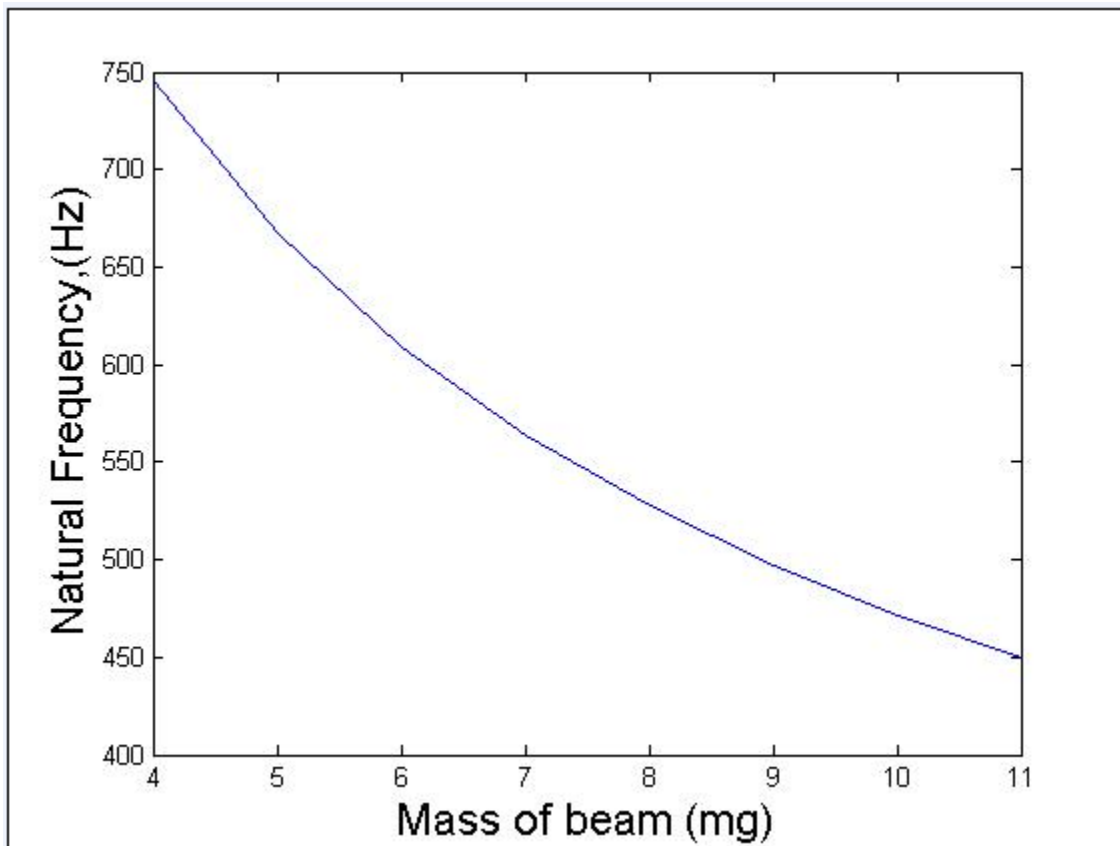


Fig21: Graph showing the variation of Natural Frequency with change in the mass of the beam

The following graphs show how the thickness of the beam will affect the maximum allowable deflection and natural frequency.

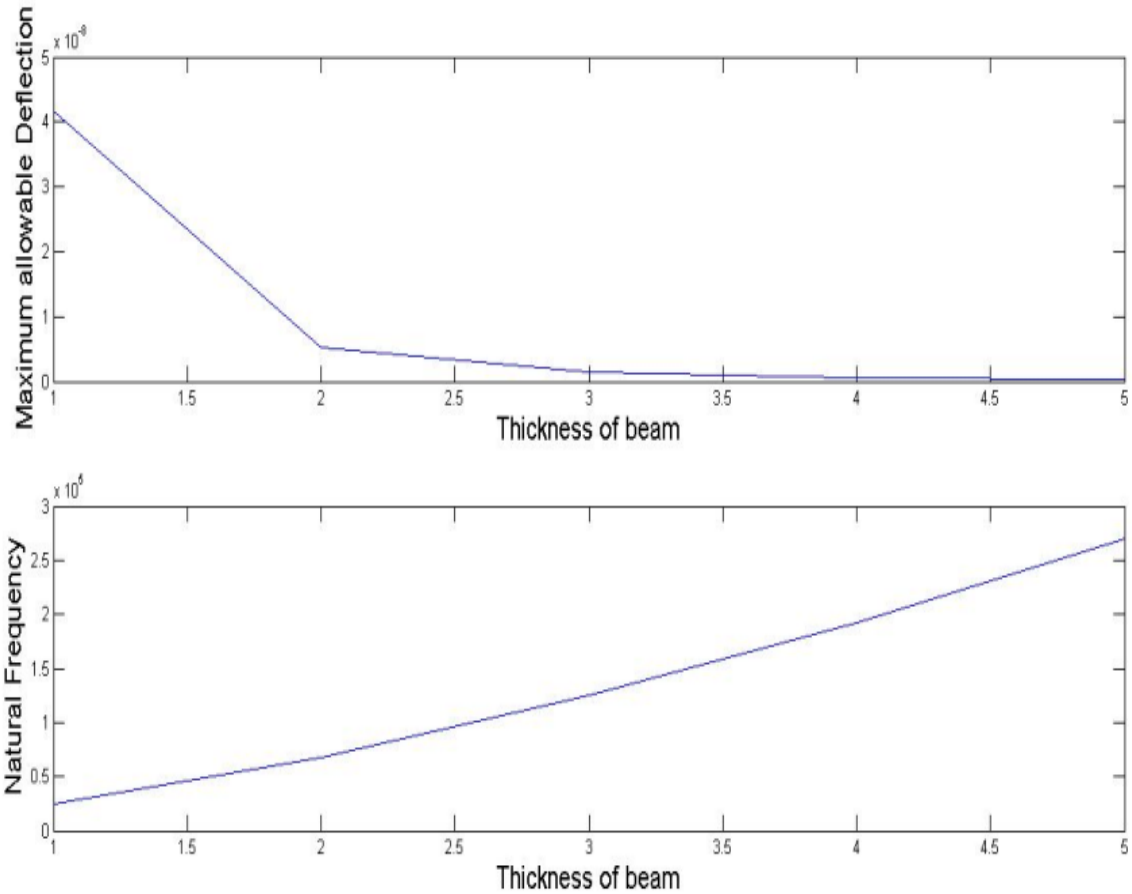


Fig22: Graphs showing variation of thickness of beam and its effect on max allowable deflection and the natural frequency

As the thickness of the beam increases, the maximum allowable deflection starts to decrease, and the natural frequency starts to increase.

The following graphs show how the width of the beam will affect the maximum allowable deflection and natural frequency.

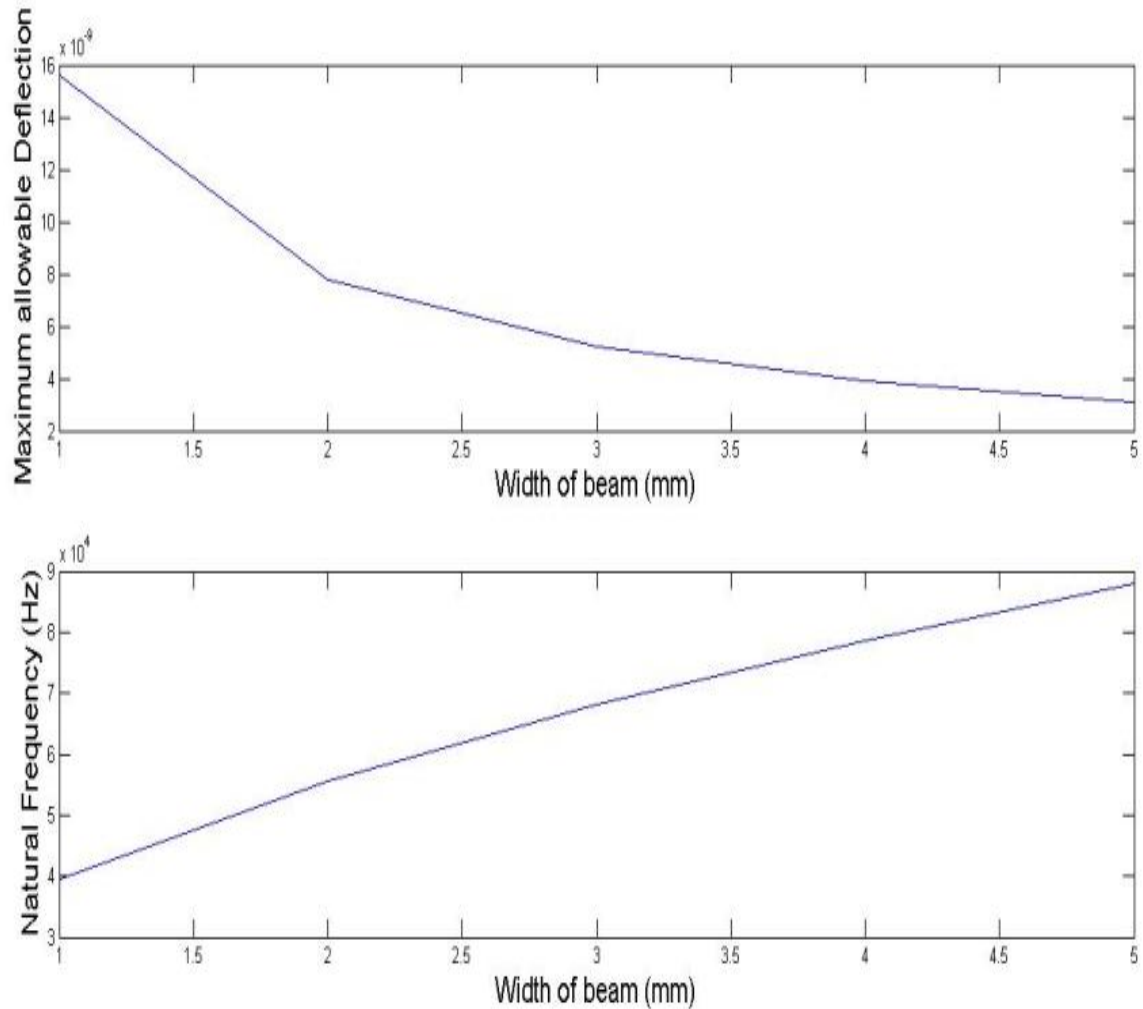


Fig23: Graphs showing variation of width of the beam and its effect on max allowable deflection and the natural frequency

As the width of the beam increases, the maximum allowable deflection starts to decrease, and the natural frequency starts to increase.

The following table summarizes how with the variation of the length of the cantilever beam, the maximum stress, deflection, spring constant and natural frequency of the beam can change. It has been summarized below: the width is 3mm, thickness 0.2mm, Young's modulus 200GPa, Vertically applied force $F = 0.005$, mass of 500mg, moment of inertia to be 2×10^{-15} are considered as constant values, calculated and mentioned above.

Table V: This table shows how the length of the beam affects the spring constant and the natural frequency of the beam, and also corresponding changes on maximum stress and deflection:

Length h L (mm)	Maximum stress $\sigma_{\max} = \frac{FLt}{2I}$	Deflection $y_{\max} = \frac{2L^2}{3Et} \sigma_{\max}$ (mm)	The spring constant $k = \frac{3EI}{L^3}$	Natural frequency $f_n = \frac{1}{2\pi} \sqrt{\frac{k}{m}}$
4	1×10^7	0.2666×10^{-5}	18750	30.516
5	1.25×10^7	0.5208×10^{-5}	9600	21.8358
6	1.5×10^7	0.912×10^{-5}	5555.5	16.611032
7	1.75×10^7	51.429×10^{-5}	3498.54	13.18198
8	2×10^7	2.133×10^{-5}	2343.75	10.78923
9	2.25×10^7	3.0375×10^{-5}	1646.09	9.041944
10	2.5×10^7	4.167×10^{-5}	1200	7.72014
11	2.75×10^7	5.545×10^{-5}	901.58	6.69171

The following table summarizes how with the length of the beam held constant at 8mm, but mass varied will affect the spring constant and the natural frequency:

Table VI: Table showing variation of spring constant and natural frequency as mass of the beam changes:

Mass M (mg)	The spring constant $k = \frac{3EI}{L^3}$	Natural frequency $f_n = \frac{1}{2\pi} \sqrt{\frac{k}{m}}$ Hz
490	2343.75	11.0072
495	2343.75	10.95148
500	2343.75	10.89659
505	2343.75	10.8525
510	2343.75	10.78923
520	2343.75	10.68498
530	2343.75	10.5837
540	2343.75	10.4852
530	2343.75	10.3894

6.2: Conversion Section:

The conversion section deals with the mechanical to electrical conversion process.

Assuming the generator is driven by a harmonic excitation, $\mathbf{y} = \mathbf{Y} \sin \omega t$ it will move out of phase with the mass resulting in a net displacement $z(t)$ between the mass and the frame while vibrating at resonance frequency.

The power extracted by the transducer mechanism and the power lost through parasitic damping, that is, the average power dissipated can be represented by:

$$P_{av} = \frac{m\xi_T Y^2 \left(\frac{\omega}{\omega_n}\right)^3 \omega^3}{\left[1 - \left(\frac{\omega}{\omega_n}\right)^2\right]^2 + \left[2\xi_T \left(\frac{\omega}{\omega_n}\right)\right]^2}$$

Where,

$\xi_T = \frac{c_T}{2m\omega_n}$, is the total damping ratio.

For steady state conditions,

P_{av} = Kinetic supplied per second by the applied vibration.

Also maximum power dissipation will occur at natural frequency (ω_n), therefore,

$$P_{av} = \frac{mY^2\omega_n^3}{4\xi_T}$$

From here it can be determined that:

- Power varies linearly with mass.
- Power increases within the cube of frequency.
- Power increases with the square of base amplitude.

If peak acceleration, $A = \omega^2 Y$ and the Damping factor $c_T = 2m\omega_n \xi_T$, then,

$$P_{av} = \frac{(mA)^2}{2c_T}$$

All the mechanical energy that is transducers into the electrical domain is not be delivered into the load.

Some of the power delivered in the electrical domain, in the case of electromagnetic transduction, is lost within the coil. The actual power in the coil is thus a function of the coil and load resistance:

$$P_{L \max} = \frac{mY^2 \omega_n^3}{16\xi_P} \left(\frac{R_{load}}{R_{load} + R_{coil}} \right)$$

Simulating the conversion section:

For the conversion from mechanical to electrical, the equations have been derived. Using suitable values, the output power equation has been simulated for varying values of damping factor.

$$P_{avelec} = \frac{mY^2\omega_n^3}{16\xi_p}$$

The graph has been shown below.

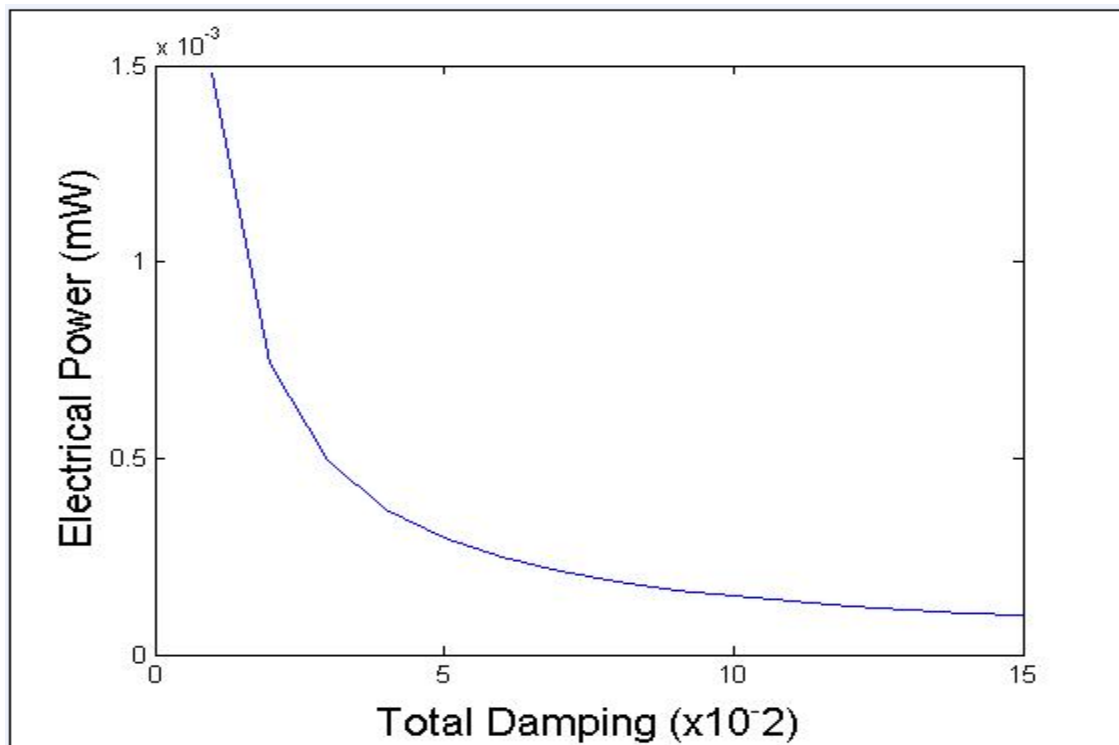


Fig24: Graph showing variation of output power with varying damping factor

The y-axis shows the output power in the mw range, and the x-axis shows the damping factor as it varies. The pattern shown in the graph states that as the damping factor increases with time, the output power generated by the energy harvester will continue to decrease.

This supports the theory that damping, both parasitic as well as electrical is not beneficial for the output power.

The second graph here shows the variation of output power vs. mass of the cantilever and the magnet. The y axis shows the output power in arbitrary units of watts, and the x axis shows the mass in arbitrary units of kg.

Visible pattern from the graph depicts that with the increase in mass the output power tends to decrease. Though at first impression, analysis of the equation may lead us to think that power should increase with mass, it is not the case, because as the mass increases, the damping and frequencies are altered.

A heavy cantilever beam will naturally undergo less displacement when placed under vibration. Hence the graph is as follows:

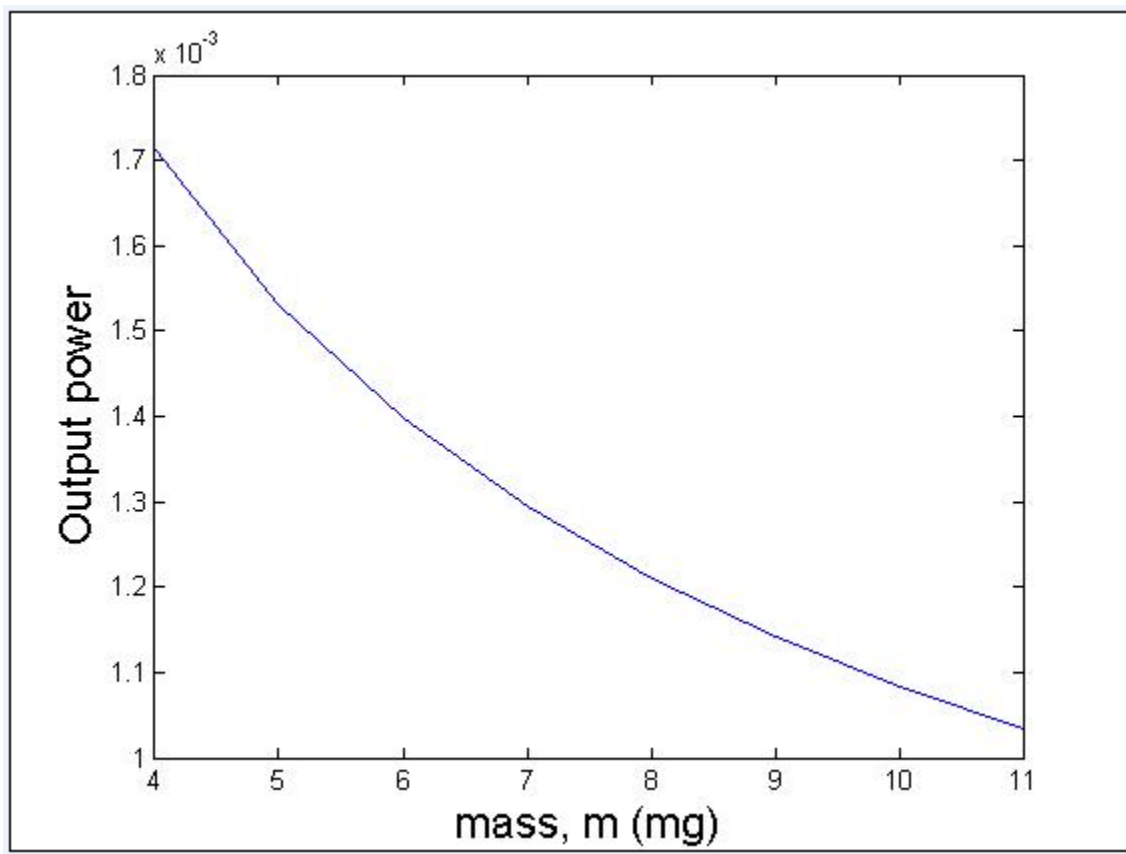


Fig 25: Variation of output power with change in mass

The graphs below show how the electrical damping is affected with variation of the coil resistance as well as the no. of turns.

The first graph shows the variation of electrical damping with coil resistance. As the coil resistance increases the electrical damping decreases.

The second graph shows that as the no. of turns increases the electrical damping increases.

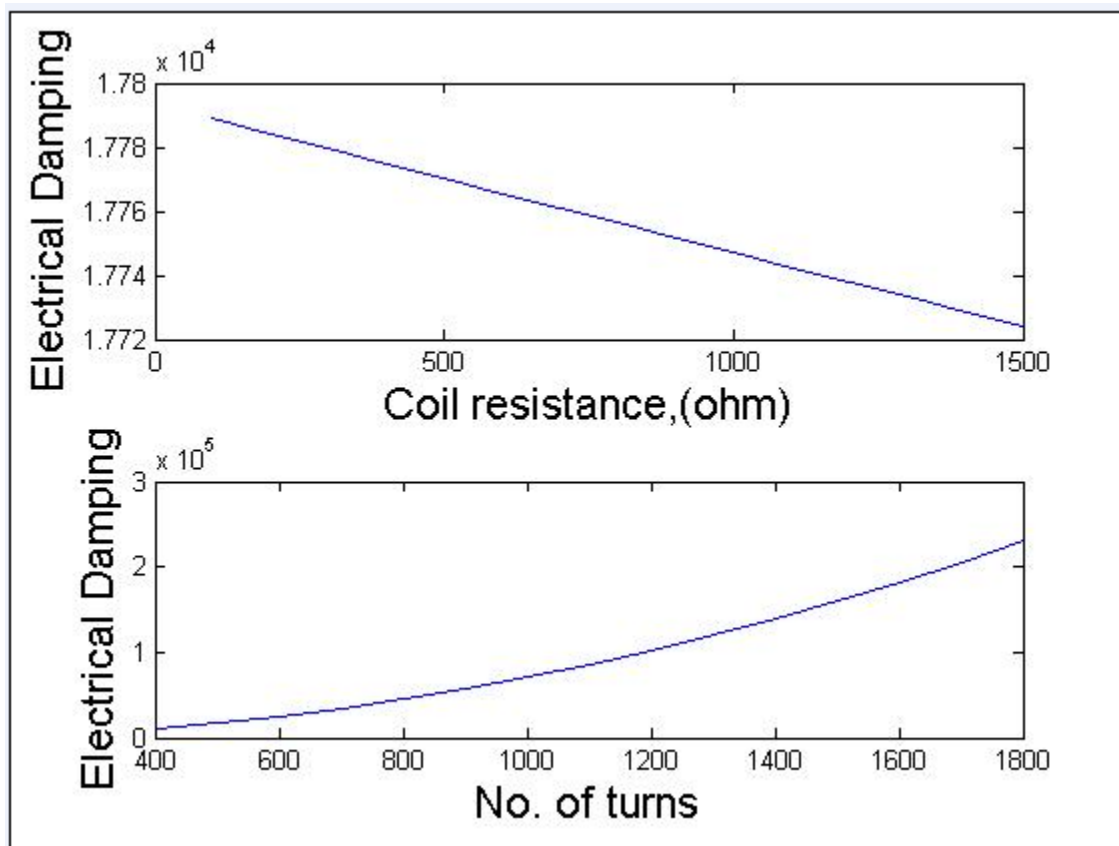


Fig26: Variation of electrical damping with (a) Coil Resistance & (b) No. of turns

The graphs below show how electrical damping is affected by variation of coil length and magnetic flux.

The simulation carried out has presented similar graphical pattern for both the variation, showing an increase in electrical damping as the coil length and magnetic flux increases.

For the generator to be constructed we want low damping values.

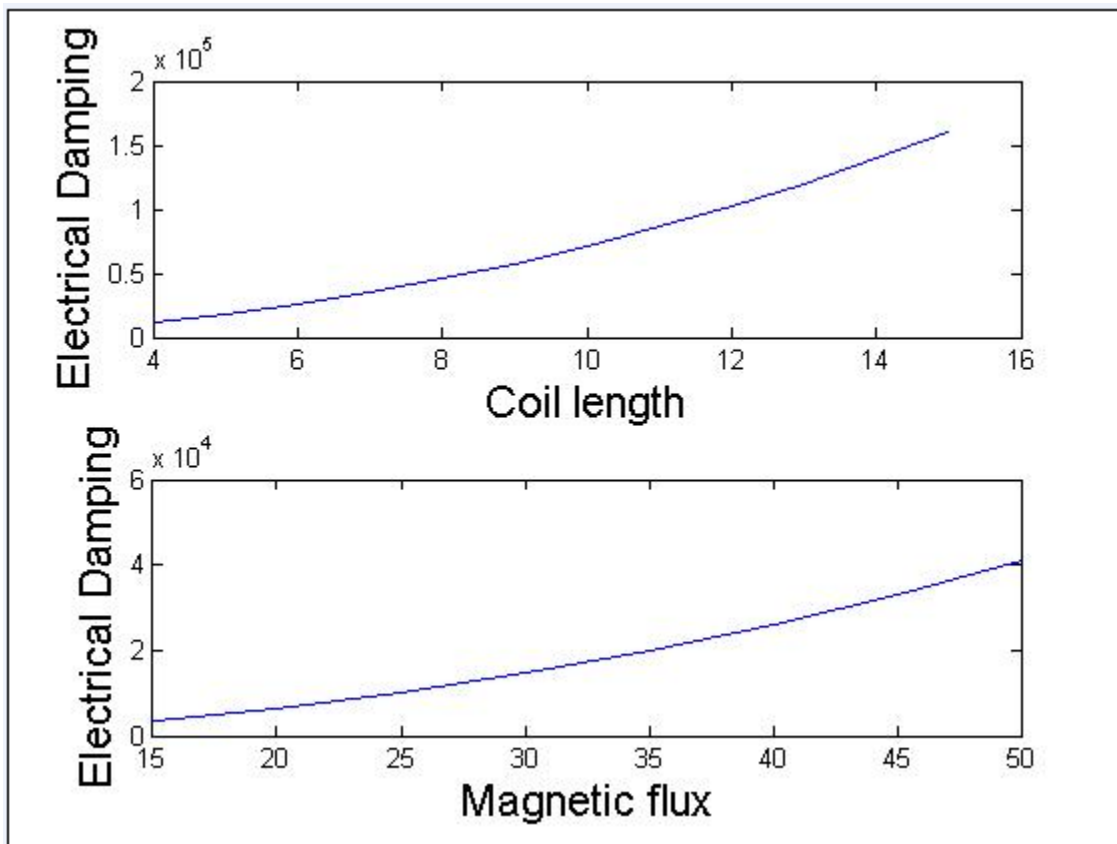


Fig27: Variation of electrical damping with (a) Coil Length & (b) Magnetic Flux

6.3: Output Section:

Once the mechanical part of the generator has been modeled and the conversion process is done, the power from the vibrations is dissipated to the electrical circuit.

This is the part of generator that the consumer side will see. Any kind of low power load device connected to it may be driven using the power dissipated from the mechanical side.

To see the variation of power or any other parameter with respect to the type of loads applied, the following simulation has been done.

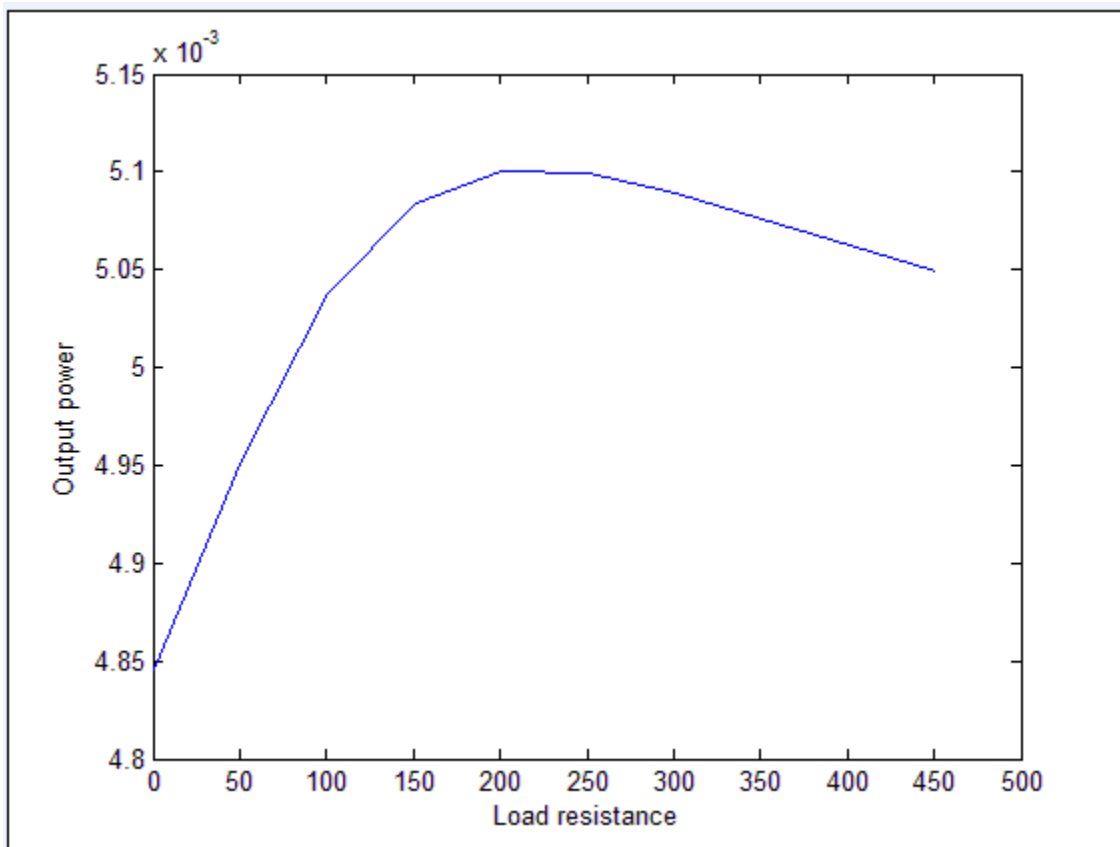


Fig28: Graph showing variation of output power with varying load resistances

The pattern shown in the graph clearly illustrates that as the load is applied in the system, the output power tends to increase, and as load linearly keeps increasing, so does output power, at one point a maximum power is reached and then the graph starts decreasing trend.

7. Estimated Design Specification for Optimum Energy Harvesting:

Table VII: The optimized device specifications:

Device Parameter	Optimized Specification
Amplitude of vibration	25 μm
Frequency of vibration	320 Hz
Length of cantilever beam	11 mm
Width of cantilever beam	3 mm
Thickness of cantilever beam	0.2 mm
Mass	510 mg
Total Damping	0.013
Type of Wire	Enameled Copper Wire
Coil Resistance	0.28 Ω
No. of turns	3 layers, each containing 9 turns
Wire Diameter	0.2 mm
Fill Factor	0.67
Load Resistance	1000 Ω
Maximum Power	124 mW
Average Power	498 mW
Magnet Specification	Mild Steel with flux density = 1.6 Tesla
Volume	240 cm^3

8. Efficiency:

The efficiency is defined as the ratio of electrical output power to absorbed mechanical power. The efficiency of this harvester is given by:

$$\eta = \frac{R_L m k_{em}^2 ((\omega_0^2 - \omega^2)^2 + (2 \zeta_m \omega_0 \omega)^2)}{\omega \left[m^2 ((R_L + R_i)^2 + (L \omega)^2) (\omega_0^2 - \omega^2)^2 + \omega^2 (k_{em}^2 + 2m\omega_0 \zeta_m \sqrt{(R_L + R_i)^2 + (L \omega)^2})^2 \right]}$$

The efficiency of electromagnetic vibration harvesters depends upon the intrinsic and extrinsic parameters like the excitation frequency or the load resistance.

Simplifying this equation we obtain a linear relationship between the efficiency and the mechanical damping ratio. High mechanical damping ratio leads to high efficiency. The increase of the efficiency is simply due to the stronger decrease of the absorbed mechanical power than the decrease of the electrical output power. The absorbed mechanical and electrical output power decrease when the mechanical damping increases, but the decrease of the electrical output power is smaller than the decrease of the absorbed mechanical power. This effect leads to high efficiency.

If $\omega = \omega_0$ and $R_L + R_i \gg L \omega$, the efficiency becomes

$$\eta = \frac{2 R_L \zeta_e \zeta_m^2}{(R_L + R_i) (\zeta_e + \zeta_m)^2}$$

Neglecting the coil resistance and setting the electromagnetic damping ratio equal to the mechanical damping ratio:

$$\begin{aligned} \eta &= \frac{\zeta_m}{2} \\ &= 0.013/2 \\ &= 0.65 \% \end{aligned}$$

9. Conclusion:

This thesis intended to explore into the possibility of designing an efficient energy harvester which can be used to drive a low power electronic device.

The designing is based on performing simulation using the software PSpice as well as MATLAB to obtain variation criteria of the device parameters.

The aim of our work is to make the energy harvester produce maximum power output in the most effective way.

10. Further Work (Future Plan):

This thesis has revealed several potential areas of research which remain open for further investigation.

- One of the requirements of traditional power processing circuitry is the need for both capacitors and inductors.
- Integrating magnetic components onto silicon is itself a major research area and
- Increasing the inductance of on-chip inductors while maintaining high Q-factors would increase the power processing efficiency of the overall system.

A lot more work can still be done.

- Application of different types of load, for ex R-L load, R-L-C load, and finally a fully operating low power device will be tried to be run using this generator ratings.
- Further optimization of the equations to try and get a higher output power density.
- The battery charger circuit will be explored to try to propose a means of running a low power device on our target application.

Reference:

- I. “A micro electromagnetic generator for vibration energy harvesting” by SP Beeby, RN Torah, MJ Tudor, P Glynn-Jones, TO’Donnell, CR Saha and S Roy; from the Journal of Micromechanics and Microengineering, 17 (2007) 1257-1265
- II. “Energy harvesting vibration sources for microsystems applications” by SP Beeby, MJ Tudor and NM White; from the journal of Measurement Science and Technology 17 (2006) R184-186
- III. “Whole Body Vibration Analysis for bus drivers” by Ana Picui; from SISOM 2009 and Session of the Commission of Acoustics, Bucharest 28-29 May
- IV. “Design and Fabrication of a new vibration-based electromechanical power generator” by M.EL-Hami, P.Glynn-Jones, N.M.White, M.Hill, S.Beeby, E.James, A.D.Brown,J.N.Ross
- V. “Cantilever Beam Analysis” – google.com
- VI. “On the effectiveness of Vibration-based energy harvesting” by Shad Roundy; from the Journal of Intelligent Material Systems and Structures, Vol.16 – October 2005, 809, 816-822
- VII. “Optimization of an Electromagnetic Energy Harvesting Device” by Chitta Ranjan Saha, Terence O’Donnell, Heiko Loder, Steve Beeby, and John Tudor; from IEEE Transactions on Magnetics, Vol.42, no.10, October 2006
- VIII. “First Draft of Standard on Vibration Energy Harvesting” from the 2nd Annual Energy Harvesting Workshop, Jan 30-31, 2007

- IX. “Electromagnetic generator for harvesting energy from human motion” by C.R.Saha, T.O’Donnell, N.Wang, P.McCloskey; from Sensors and Actuators A:Physical
- X. “Analogous Electrical Circuit of Suspension System” by Eng. Fuad Rajab
- XI. D. M. ROWE, D. V. MORGAN and J. H. KIELY, “Low cost miniature thermoelectric generator”. Electron. Lett. 27, 1991, pp. 2332-2334.
- XII. T. STARNER, “Human powered wearable computing”. IBM Syst. J., Vol. 35, Nos. 3-4, 1996, pp. 618-629.
- XIII. M. HAYAKAWA, “Electronic wristwatch with generator”. US patent 5001685, 1991
- XIV. <http://www.techeblog.com/gadged>
- XV. Energy harvesting/scavenging ,paul wright ,ITIRS, 2006.
- XVI. Green integration: <http://www.gearfuse.com/hymini-wind-powered-device-charger-puts-the-green-in-awesome/>
- XVII. F. Moll and A. Rubio, “An approach to the analysis of wearable body-power systems,” in *Mixed Signal Design Workshop, MIXDES’00*, 2000.

- XVIII. P. D. Mitcheson, T. C. Green, E. M. Yeatman, and A. S. Holmes, "Architectures for vibration-driven micropower generators," *J. of Microelectromechanical Systems* 13, June 2004.
- XIX. Review of Energy Harvesting Techniques and Applications for Microelectronics, Loreto Mateu and Francesc Moll Universitat Politècnica de Catalunya Dept. of Electronic Engineering Barcelona, Spain
- XX. Serre C et al Vibrational Energy Scavenging with Si-Technology
Eelectromagnetic Inertial Microgenerators *DTIP of MEMS & MOEMS2006*
- XXI. Bouendeu E et al Design synthesis of electromagnetic vibration-driven energy generators using a variational formulation *JMEMS* (submitted on 6th June 2009)
- XXII. P. Mitcheson, B.P. Stark, E. Yeatman, A. Holmes, T. Green, Analysis and optimization of MEMS on-chip power supply for self powering of slow moving sensors, in: Proc. Eurosensors XVII (2003).
- XXIII. Challa, V.,R., Prasad, M.,G., Shi, Y., Fisher, F.,T., " A wide frequency range tunable vibration energy harvesting device using magnetically induced stiffness", Proceedings of IMECE07, 41985: P. 1-9, 2007.
- XXIV. Beeby, S.,P., Tudor, M.,J., White, N.,M., " Energy harvesting vibration sources for microsystems applications", Measurement Science and Technology, 17: P. R175-R195, 2006.
- XXV. Beeby, S.P., Tudor, M.J., Koukharenko, E., White, N.M., O'Donnell, T., Saha, C., Kulkarni, S.Roy, S., "Design, fabrication and simulations of micro electromagnetic vibration-powered generator for low power MEMS", DTIP of MEMS and MOEMS", Montreux, Switzerland, 2005.

Appendix:

1. [XXI]

Characteristics of commonly occurring vibration sources

Vibration sources	Peak acceleration [ms ⁻²]	Frequency of peak acceleration [Hz]
Base of 5HP 3-axis machine tool with 36'' bed	10	70
Kitchen blender casing	6.4	121
Clothes dryers	3.5	121
Door frames just after door closes	3	125
Small microwave oven	2.25	121
HVAC vents in office building	0.2 – 1.5	60
Wooden deck with people walking	1.3	385
Bread maker	1.03	121
External window (60cm x 90cm) next to a busy street	0.7	100
Notebook computer while CD is being read	0.6	75
Washing machine	0.5	109
Second story floor of a wood frame office building	0.2	100
Refrigerator	0.1	240
Shake-driven flashlight	12.8	3.3
AC-synchronous motor running at 50Hz	0.34 – 9.82	100
Rotor blade for helicopter	0.34	17.2
Power transformer running at 50Hz	0.12*, 0.39**, 0.73***	100
Into a pocket of a walking man	0.31	2
Running man onto stairs	0.91	10
Into a woman bag	0.43	2
Car Instrument panel	3	13
Car engine	12	200
Front glass of a car	0.14	15
Guard rail near a busy street	0.01	50
Blender casing	6.4	121
Clothes dryer	3.5	121
Door frame just after door closes	3	125

* Normal, ** partially loosened, *** wholly loosened

2. Table showing common coil materials and their properties:

Material	Thermal expansion coefficient [1/K]	Density [kg/m ³]	Resistivity [Ωm]
Copper	16.5x10 ⁻⁶	8960	17.2x10 ⁻⁹
Alumimium	23.1x10 ⁻⁶	2700	28.1x10 ⁻⁹
Silver	18.9x10 ⁻⁶	10500	16.2x10 ⁻⁹
Gold	14.2x10 ⁻⁶	19300	22x10 ⁻⁹

3. Guide for construction on PCB:

(a) Table: Type of application and the configuration required:

Type of application	Type of configuration	
Small area application	Standard configuration <ul style="list-style-type: none"> • Cantilever-like • S-shaped • Circular • Beam-like 	Inverse configuration <ul style="list-style-type: none"> • Cantilever-like • S-shaped • Circular ✓ Circular coil ✓ Square coil ✓ Meandering coil ✓ Solenoid-like coil
Large area application	Standard configuration <ul style="list-style-type: none"> • Circular • Butterfly-like 	

(b) Table: The type of data required:

Load requirement	Design constraint	Degree of freedom of designer
<ul style="list-style-type: none">• Output power• Load voltage	<ul style="list-style-type: none">• Excitation frequency• Excitation amplitude• Proof mass• Overall bandwidth• Total size or weight of the harvester	<ul style="list-style-type: none">• Resistivity of the wire of the coil• Wire diameter or cross section area• Wire length• Mechanical damping ratio

4. Coding Data:

The Codes for the simulation are as follows:

Power relation:

```
1) Y=25*10^(-6);
2) k=901.58;
3) c=0.013;
4) m=0.510;
5) Rload=500;
6) Rcoil=0.28;
7) Pavelec=[];
8) Plmax=[];
9) ztap=[];
10) i=1;
11) for p= 9:1:15
12)     wn=sqrt(k/m);
13)     ztap(i)= p*10^(-3);
14)     Pavelec(i)=(m*wn^3*Y^2)/(16*ztap(i));
15)
    Plmax(i)=[(m*wn^3*Y^2)/(16*ztap(i))]*[(Rload)/(Rload+Rcoil)];
```

```

16)     i=i+1;
17) end
18)
19) subplot(211), plot(ztap,Plmax),xlabel('Damping
      Factor'),ylabel('Output power');
20)
21)
22) subplot(212), plot(ztap,Pavelec),xlabel('Damping
      Factor'),ylabel('avarege electromagnetic power');

```

Simulation for cantilever beam:

```

F=0.005;
%%m=5.1*10^(-4);
E=2*(10^11);
t=0.2;
W=3;
y=[];
fn=[];
i=1;
k=[];
for L= 4:1:11
    I=(W*t^3)/12
    U=(F*L*t)/(2*I)
    y(i)=(2*L*L*U)/(3*E*t)

    k(i)=(3*E*I)/L^3

    i=i+1;
end
j=1;
for m= 4:1:11
    fn(j)=(1/2*pi)*(sqrt(k(j)/(m*10^(-4))))
    j=j+1;
end

```

```

L= 4:1:11;
subplot(311), grid on,plot(L,y),xlabel('Length of
beam'),ylabel('Maximum allowable Deflection');
subplot(312),plot(L,fn),xlabel('Length of beam'),ylabel('Natural
Frequency');
m= 4:1:11
subplot(313),plot(m,fn),xlabel('Mass of beam x 10^(-
4)'),ylabel('Natural Frequency');

```

Thickness:

```

F=0.005;
m=5.1*10^(-4);
E=2*(10^11);
L=5;
W=3;
y=[];
fn=[];
i=1;
for t= 1:1:5
    I=(W*(t*10^(-1))^3)/12
    U=(F*L*(t*10^(-1)))/(2*I)
    y(i)=(2*L*L*U)/(3*E*(t*10^(-1)))

    k=(3*E*I)/L^3
    fn(i)=(1/2*pi)*(sqrt(k/m))

    i=i+1;
end
t= 1:1:5;
subplot(211), grid on,plot(t,y),xlabel('Thickness of
beam'),ylabel('Maximum allowable Deflection');
subplot(212),plot(t,fn),xlabel('Thickness of beam'),ylabel('Natural
Frequency');

```

Width:

```
F=0.005;
m=5.1*10^(-4);
E=2*(10^11);
L=5;
t=0.2;
y=[];
fn=[];
i=1;
for w=1:1:5
    I=(w*t^3)/12
    U=(F*L*t)/(2*I)
    y(i)=(2*L*L*U)/(3*E*t)

    k=(3*E*I)/L^3
    fn(i)=(1/2*pi)*(sqrt(k/m))

    i=i+1;
end
w= 1:1:5;
subplot(211), grid on,plot(w,y),xlabel('Width of beam'),ylabel('Maximum
allowable Deflection');
subplot(212),plot(w,fn),xlabel('Width of beam'),ylabel('Natural
Frequency');
```

Simulation for Average Power and Natural Frequency:

```
Y=25*10^(-6);
F=9.8*0.510;
f=327;
w=2*pi*f;
Dt=0.013;
k=901.58;
```



```

Pav=[];
a=[];
wn=[]
i=1;
for m= 5:1:15
    a(i)=m*10^(-4);
    wn(i)=sqrt(k/a(i));
    zmax=(F+(a(i)*w^2*Y))/(Dt*w);
Pav(i)=(a(i)*wn(i)^3*Y*zmax)/(2);
i=i + 1;
end
m= 5:1:15
subplot(211), plot(m,wn),ylabel('Natural Frequency'),xlabel('Mass of
the beam');
subplot(212),plot(a,Pav),ylabel('Average Power'),xlabel('Mass of the
beam');

```

Simulation for Maximum power:

```

Y=25*10^(-6);
k=901.58;
c=0.013;
%m=5.1*10^(-4);
ztap= 9.59*10^(-3);
Rcoil=0.28*64;
Pavelec=[];
Plmax=[];
Rload=1000;
wn=[];
i=1;
j=1;
for m= 4:1:11

```

```

    wn=sqrt(k/m)

    Plmax(j)=[(m*10^(-
4)) *wn^3*Y^2)/(16*ztap)]*[(Rload)/(Rload+Rcoil)];

    j=j+1;
end
m= 4:1:11
plot(m,Plmax),xlabel('mass x 10^(-4)'),ylabel('Output
power');

```

Simulation for Average Power and Maximum Power with respect to Total Damping:

```

Y=25*10^(-6);
F=9.8*0.510;
f=327;
w=2*pi*f;
Dt=0.013;
k=901.58;
Rload=1000;

Plmax=[];
Pav=[];
a=[];
Ct=[];
wn=[];
zta=[];
i=1;
for m= 5:1:15
    a(i)=m*10^(-4);
    wn(i)=sqrt(k/a(i));
    zmax=(F+(a(i)*w^2*Y))/(Dt*w);
    Pav(i)=(a(i)*(wn(i)^3)*Y*zmax)/(2);

```

```

i=i + 1;
end
i=1;
for m=5:1:15
A=(w^2)*Y;
Ct(i)=(m*A)^2/(2*Pav(i));
i=i+1;
end
plot(Ct,Pav),xlabel('Total Damping'),ylabel('Average Power')
j=1;
for m= 5:1:15
    zta(j)= Ct(j)/(2*a(j)*wn(j));
    j=j+1;
end
i=1;
for Rcoil= 100:100:1100
    Plmax(i)=
[(a(i)*Y^2*wn(i)^3)/(16*zta(i))]*[Rload/(Rload+Rcoil)];
    i=i+1;
end

m= 5:1:15
plot(zta,Plmax),xlabel('Damping ratio'),ylabel('Maximum Power');

```

Electrical Damping

```

N=500,
l=5;
B=33;
Rl=1000;
Rc=100;
Lc=23;
f=233;
w=2*pi*f;
Ce=[];
Cei=[];
a=1;

```

```

for Rc=100:100:1500
    Ce(a)=(N*l*B)^2/(Rl+Rc+(Lc*j*w));
a=a+1;
end
Rc=100:100:1500
subplot(411),plot(Rc,Ce),xlabel('Coil resistance'),ylabel('Electrical
Damping');

Rc=100;
a=1;
for N=400:100:1800
    Ceii(a)=(N*l*B)^2/(Rl+Rc+(j*Lc*w));
a=a+1;
end
N=400:100:1800
%subplot(412),plot(N,Ceii),xlabel('No. of turns'),ylabel('Electrical
Damping');

N=500;
Ceii=[];
a=1;
for l=4:1:15
    Ceiii(a)=(N*l*B)^2/(Rl+Rc+(j*Lc*w));
a=a+1;
end
l=4:1:15
subplot(211),plot(l,Ceiii),xlabel('Coil length'),ylabel('Electrical
Damping');

l=5;
Ceiii=[];
a=1;
for B=15:5:50
    Ceiiii(a)=(N*l*B)^2/(Rl+Rc+(j*Lc*w));
a=a+1;
end
B=15:5:50

```

```
subplot(212),plot(B,Ceiii),xlabel('Magnetic flux'),ylabel('Electrical  
Damping');
```

Relation of z:

```
Y=25*10^(-6);  
F=9.8*0.510;  
f=327;  
w=2*pi*f;  
Dt=0.013;  
k=901.58;  
Pav=[];  
a=[];  
wn=[]  
zmax=[]  
i=1;  
for m= 5:1:15  
    a(i)=m*10^(-4);  
    wn(i)=sqrt(k/a(i));  
    zmax(i)=(F+(a(i)*wn(i)^2*Y))/(Dt*wn(i));  
Pav(i)=(a(i)*wn^3*Y*zmax)/(2);  
i=i + 1;  
end  
m= 5:1:15  
plot(wn,zmax),xlabel('Wn'),ylabel('Displacement of the beam');  
plot(m,wn),ylabel('Natural Frequency'),xlabel('Mass of the beam');  
plot(a,Pav),ylabel('Average Power'),xlabel('Mass of the beam');
```